Available online at www.sciencedirect.com
SCIENCE DIRECT
ELSEVIER
Coordination Chemistry Reviews 250 (2006) 1152–1177
COORDINATION CHEMISTRY REVIEWS
www.elsevier.com/locate/ccr

Review

Metal complexes of chelating diarylamido phosphine ligands

Lan-Chang Liang *

Department of Chemistry and Center for Nanoscience & Nanotechnology, National Sun Yat-sen University, Kaohsiung 80424, Taiwan

Received 31 December 2005; accepted 3 January 2006
Available online 7 February 2006

Contents

Abstract

This review summarizes the recent progress in coordination and organometallic chemistry involving metal complexes of chelating diarylamido phosphine ligands, including bidentate amido phosphine $[NP]^-$, tridentate amido diphosphine $[PNP]^-$, and tridentate diamido phosphine $[NPN]^{2-}$. Consistent with the anticipated hybrid characteristic of the ligands, diarylamido phosphine complexes that have been characterized thus far involve both soft and hard main-group and transition metals. The inherent rigidity and robustness imposed by the *o*-phenylene backbone of the ligands are beneficial to the development of reaction chemistry of these diarylamido phosphine complexes. Preparation of the ligand precursors and the corresponding metal complexes and the subsequent reactivity studies are discussed.

Keywords: Amido phosphine ligands; Diarylamido phosphine ligands; Hybrid ligands; Main-group metal; Pincer ligands; Transition metal

* Tel.: +886 7 5252000x3945; fax: +886 7 5253908.
E-mail address: lcliang@mail.nsysu.edu.tw.

0010-8545/$ – see front matter © 2006 Elsevier B.V. All rights reserved.
doi:10.1016/j.ccr.2006.01.001

1. Introduction

The search for appropriate ligand sets that effectively control the stability and reactivity of metal complexes continues to play an essential role in inorganic and organometallic chemistry. Hybrid chelating ligands that contain both soft and hard donor atoms are currently receiving increasing attention due to their potentials for generating metal complexes with unusual reactivity [1]. One remarkable precedent in this aspect is the chelating amido phosphine ligands that incorporate the $-SiMe_2CH_2-$ backbone (Fig. 1) [2–15]. These compounds have shown widespread reactivity with metals across the periodic table. Significant results have evolved extensively in the last 25 years. Of particular note is the successful hydrogenation of coordinated dinitrogen molecules [1,16–18]. One notable drawback in this ligand system, however, is perhaps the participation of the $-SiMe_2CH_2-$ backbone under certain circumstances [19]. In particular, cleavage of both N–Si [20,21] and C–H [22] bonds has been observed.

Recent progress in the amido phosphine chemistry has emerged considerably with the employment of ligands that contain the *o*-phenylene-derived backbone. In particular, metal complexes of diarylamido phosphine ligands are currently under extensive investigation. It was reasoned [23] that ligands of this type are relatively more rigid and robust than those of the $-SiMe_2CH_2-$ derivatives, thus holding the promise to diminish the possibility of undesired reactivity involving the amido phosphine ligands. It should be noted that although *o*-phosphinoaniline and its *N*-alkylated (usually small or primary alkyls) compounds are popular ligands in the last 40 years [24–27], the *o*-phosphine functionalized diarylamine derivatives are notably unknown until 2003 [23,28,29]. This review attempts to give a comprehensive coverage of the literature in this rapidly expanding area. Any omissions are unintentional. Though developed only recently, there have been three types of diarylamido phosphine ligands reported to date. Fig. 2 illustrates the bi- and tridentate ligands of *o*-phenylene derivatives that are analogous to those containing the $-SiMe_2CH_2-$ backbone as shown in Fig. 1.

The chelating diarylamido phosphine ligands depicted in Fig. 2 are intriguing for several reasons. First, with the hybrid characteristic, these compounds are suitable ancillary ligands for both hard and soft metals on the basis of the hard and soft acids and bases (HSAB) theory [30]. It has been shown in the silyl-derived ligand system that the apparent mismatch of the hard–soft donor–acceptor pairs in the amido phosphine complexes facilitates the isolation of otherwise inaccessible reactive species [1], although the activation of the hybrid ligand itself may occasionally become problematic [20–22]. Utilization of

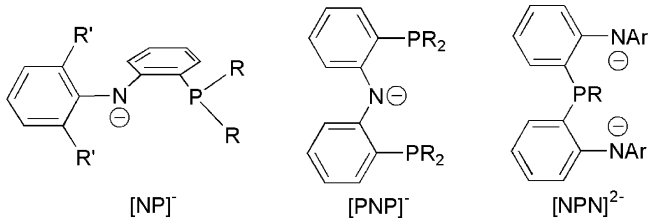

Fig. 2. Representative diarylamido phosphine ligands.

the *o*-phenylene backbone in the chelating amido phosphine ligands is beneficial in view of the relatively robust N–C_{sp^2} bonds as compared to the N–Si bonds. The rigidity imposed by the *o*-phenylene backbone simultaneously inhibits donor atom dissociation from the metal center, at least to some degree, thus possibly enhancing the thermal stability of the metal complexes in comparison with those of the silyl derivatives. Second, these diarylamido phosphine ligands are extremely versatile given a number of parameters available for the constitution of this ligand set, including variable hapticities, formal charges, and substituents at the donor atoms, etc. The reactivity and stability of the diarylamido phosphine complexes are thus finely tunable. Third, in addition to the resemblance to those shown in Fig. 1, the representative examples illustrated in Fig. 2 fall into the category of several popular motifs of ligand design that effectively controls the reactivity and structure of the metal complexes. As a result, direct comparisons of chemistry derived from these related but inherently different ligand systems are particularly valuable. For instance, metal complexes of the monoanionic $[NP]^-$ and $[PNP]^-$ ligands can be regarded as one of the variations of the popular phosphine metallacycles [31–33]. In particular, the meridional $[PNP]^-$ represents one of the $[LXL]^-$ (L = P, N, S, etc.; X = N, C, etc.) pincer ligands [34–39]. The dianionic $[NPN]^{2-}$ resembles other diamido/donor ligand systems [3,40–46]. Furthermore, the incorporation of the phosphorus donor(s) in the ligand design is beneficial due, at least in part, to the facile accessibility of the ^{31}P ($I = 1/2$, natural abundance 100%) NMR handle, which has been an extremely invaluable tool for the development of the amido phosphine chemistry in terms of reaction parameter determination, intermediate and/or product characterization, and perhaps mechanistic possibility elucidation. The multiplicity of the resonances and the magnitude of the internuclear coupling constants $^nJ_{PE}$ (E = metal, donor atom, or atoms covalently bound to the donor atom; $n = 1$, 2, 3) are of particular value, e.g., $^1J_{MP}$, $^2J_{PP}$, and $^3J_{PH\alpha}$, to determine the solution structures.

Other than solution NMR spectroscopy, X-ray crystallography provides equally important evidence for the characterization of isolated compounds. Table 1 summarizes the selected spec-

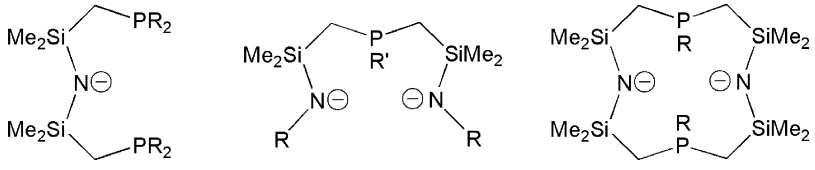

Fig. 1. Chelating amido phosphine ligands that contain the $-SiMe_2CH_2-$ backbone.

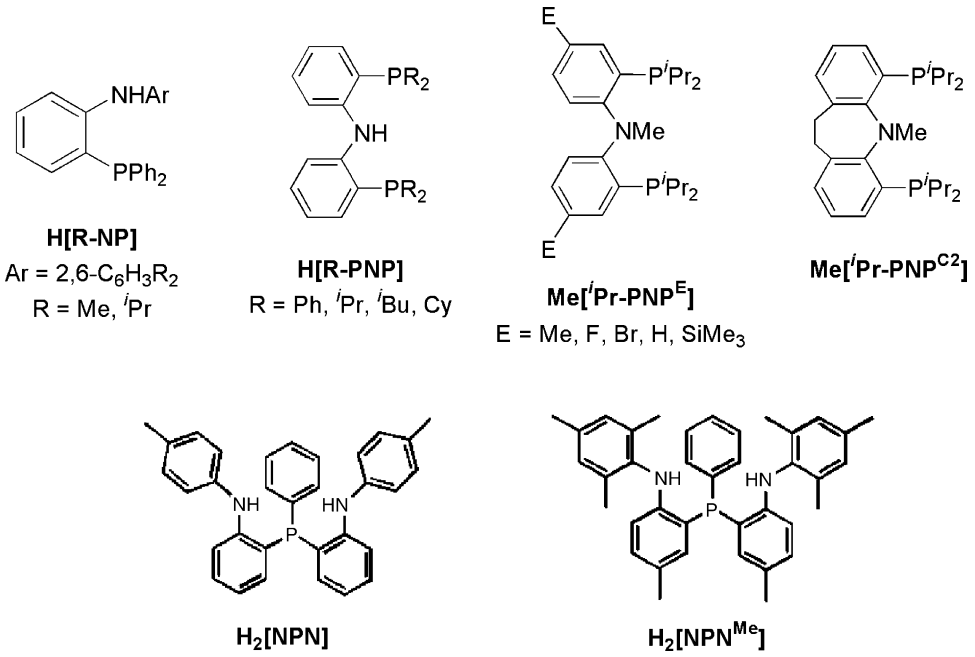

Fig. 3. Abbreviations employed for diarylamido phosphine ligand precursors.

troscopic and crystallographic data for comparison purpose. For instance, although the changes in ^{31}P chemical shifts arising from different ligand backbones (e.g., phenylene versus tolylene) are negligible, those corresponding to the variations of substituents at the donor atoms (e.g., alkyl versus aryl at P and proton versus methyl at N) alter significantly. Table 1 also serves as a quick reference guide to the literature. The abbreviations employed for ligands discussed are summarized in Fig. 3.

2. Ligand precursors

2.1. Bidentate amido phosphine ligands

Scheme 1 summarizes the preparation of the ligand precursors of this type. The synthesis is straightforward. The strategy takes advantage of the fact that aryl fluoride compounds are virtually inactive to the well-developed palladium-catalyzed aryl amination reactions [47–49] but reactive to the nucleophilic phosphanylation [50,51]. Both *N*-(2-diphenylphosphinophenyl)-2,6-diisopropylaniline (H[^{i}Pr-NP]) [28] and *N*-(2-diphenylphosphinophenyl)-2,6-dimethylaniline (H[Me-NP]) [52] were readily prepared from commercially available starting materials. Consistent with the anticipated steric size of the *ortho*-substituted aryls at the nitrogen atom, the isopropyl derivatives require relatively harsh conditions for both palladium-catalyzed cross-coupling reaction and nucleophilic phosphanylation in order for high yield isolation of the desired products as compared to their methyl analogues.

The solution and solid-state structures of both H[^{i}Pr-NP] and H[Me-NP] were investigated by multi-nuclear NMR spectroscopy and X-ray crystallography, respectively. The solution ^{1}H and ^{13}C NMR data indicate that the *ortho*-alkyl groups in these molecules are chemically equivalent. Diastereotopic isopropylmethyl groups are found for H[^{i}Pr-NP] on the basis of variable-temperature ^{1}H NMR studies. This phenomenon is ascribed to restricted rotation about the *N*-aryl bond due to steric demand of the substituent at the nitrogen atom. Consistent with these results, an X-ray study of H[^{i}Pr-NP] [53] revealed that the diisopropylphenyl group is roughly perpendicular to the *o*-phenylene backbone and the isopropylmethyl moieties are oriented such that they are tilted away from the phosphorus atom. The NH proton in both compounds was observed as one doublet resonance with J_{HP} of ca. 8 Hz.

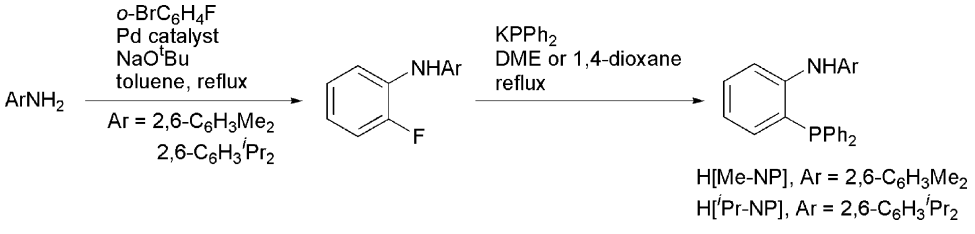

Scheme 1.

Table 1
Selected spectroscopic and crystallographic data for diarylamido phosphine complexes and the corresponding ligand precursors[a]

Compound	δ_P	$^1J_{PM}$	M—N distance (Å)	M—P distance (Å)	Reference
H[^{i}Pr-NP]	−20.1				[28]
H[Me-NP]	−19.3				[52]
H[Ph-PNP]	−18.6				[23,29,54]
H[^{i}Pr-PNP]	−13.3				[54]
H[Cy-PNP]	−22.0				[54]
H[^{i}Bu-PNP]	−54.5[b]				[55]
H[^{i}Pr-PNP^{Me}]	−12.9				[56]
Me[^{i}Pr-PNP^{Me}]	−6.8				[57]
Me[^{i}Pr-PNP^{F}]	−6.3				[58]
Me[^{i}Pr-PNP^{Br}]	−5.2				[58]
Me[^{i}Pr-PNP]	−6.4				[58]
Me[^{i}Pr-PNP^{SiMe3}]	−6.1				[58]
Me[^{i}Pr-PNP^{C2}]	−8.8				[59]
H_2[NPN]	−30.9				[60]
H_2[NPN^{Me}]	−31.4				[60]
Group 1					
[^{i}Pr-NP]Li(THF)$_2$	−12.0	38			[28]
[Me-NP]Li(THF)$_2$	−12.7[c,d]	34[c,d]	1.990(5)	2.620(5)	[53]
[Ph-PNP]Li(THF)$_2$	−13.6[c]	34[c]	2.039(5)	2.779(5) 2.824(5)	[23]
[^{i}Pr-PNP]Li(THF)	−4.0[c]	46[c]			[54]
[^{i}Pr-PNP]Li(OEt$_2$)	−4.9				[54]
[Cy-PNP]Li(THF)	−12.1	46			[54]
[Cy-PNP]Li(OEt$_2$)	−13.0		1.979(3)	2.578(3) 2.502(3)	[54]
[^{i}Pr-PNP^{Me}]Li	−4.4				[61]
[^{i}Pr-PNP^{Me}]Li(THF)	−4.1	48	1.942(6)	2.556(5) 2.531(5)	[61]
[^{i}Bu-PNP]Li	−49.4	61			[55]
[NPN]Li$_2$(THF)$_2$	−33.0	41			[60]
[NPN^{Me}]Li$_2$(dioxane)	−35.2	40			[60]
[NPN^{Me}]Li$_2$(THF)$_2$			2.078(3) 2.046(4) 2.051(3) 2.076(3)	2.510(3)	[60]
Group 4					
[^{i}Pr-PNP^{Me}]Ti(CH$_2$CMe$_3$)$_2$			2.068(2)	2.6779(9) 2.6795(9)	[62]
[^{i}Pr-PNP^{Me}]Ti(=CHCMe$_3$)(OTf)	33.6 24.2		2.034(5)	2.603(2) 2.6080(18)	[62]
[^{i}Pr-PNP^{Me}]Ti(=NAr)(CH$_2$CMe$_3$) (Ar = 2,6-C$_6$H$_3$^{i}Pr$_2$)	24.2 16.7		2.125(9)	2.568(4) 2.672(4)	[62]
[^{i}Pr-PNP^{Me}]Ti(=PAr)(CH$_2$CMe$_3$) (Ar = 2,4,6-C$_6$H$_2$^{i}Pr$_3$)	37.2 31.1		2.1023(11)	2.5947(4) 2.5681(4)	[62]
[^{i}Pr-NP]ZrCl$_3$(THF)	2.0		2.085(7)	2.786(3)	[66]
[Me-NP]$_2$ZrCl$_2$	12.3		2.132(5) 2.140(5)	2.7993(16) 2.8017(18)	[66]
[^{i}Pr-PNP^{Me}]ZrCl$_3$	27.1[e]				[61]
[^{i}Pr-PNP^{Me}]ZrMe$_3$	13.0		2.223(4)	2.7549(17) 2.7984(18)	[61]
[^{i}Pr-PNP^{Me}]Zr(CH$_2$Ph)$_3$	12.9				[61]
[^{i}Pr-PNP^{Me}]Zr(CH$_2$R)$_3$ (R = *p*-tolyl)[e]	12.2				[61]
[^{i}Pr-PNP^{Me}]Zr(=CHPh)(CH$_2$Ph)	28.6 26.6				[61]

Table 1 (*Continued*)

Compound	δ_P	$^1J_{PM}$	M—N distance (Å)	M—P distance (Å)	Reference
[^{i}Pr-PNP^{Me}]Zr(=CHR)(CH$_2$R) (R = *p*-tolyl)	28.4 27.3				[61]
[NPN^{Me}]Zr(NMe$_2$)$_2$	−11.5				[60]
[NPN^{Me}]ZrCl$_2$	−2.8		2.060(2) 2.072(2)	2.7229(8)	[60]
[NPN^{Me}]ZrCl$_2$(THF)	2.7				[60]
[NPN^{Me}]ZrMe$_2$	−14.1				[60]
[^{i}Pr-NP]HfCl$_3$(THF)	4.1				[66]
[Me-NP]$_2$HfCl$_2$	10.5		2.127(3) 2.127(3)	2.7736(9) 2.7736(9)	[66]
Group 8					
[^{i}Pr-PNP^{Me}]Ru(H)(H$_2$)	70.8				[70]
[^{i}Pr-PNP^{Me}]Ru(H)(CO)	67.9		2.070(3)	2.3069(11) 2.3306(11)	[70]
[^{i}Pr-PNP^{Me}]Ru(Me)(CO)	56.1				[70]
Group 9					
[Ph-PNP]Rh(H)(Cl)	35.1[f]	109[f]			[29]
[Ph-PNP]Rh(COE)	38.8	148			[29]
[Ph-PNP]Rh(CO)	41.8	135	2.074(9)	2.292(3) 2.292(3)	[29]
{H[Ph-PNP]}Rh(μ-Cl)$_2$(RhCl$_2$)	37.1[f]	116[f]			[29]
[^{i}Pr-PNP^{Me}]Rh(H)(Cl)	48.5	105			[57]
{Me[^{i}Pr-PNP^{Me}]}RhCl	32.5	154	2.134(10)	2.292(4) 2.233(4)	[57,59]
{Me[^{i}Pr-PNP^{F}]}RhCl	32.8	154			[59]
[^{i}Pr-PNP^{Me}]Rh(Me)(Cl)	36.2	109	2.059(14)	2.332(5) 2.305(5)	[57,59]
[^{i}Pr-PNP^{F}]Rh(Me)(Cl)	36.5	110			[59]
[^{i}Pr-PNP^{C2}]Rh(Me)(Cl)	42.6 36.7				[59]
{Me[^{i}Pr-PNP^{C2}]}RhCl[e]	34.4	151			[59]
{[^{i}Pr-PNP^{C2}]CH$_2$}Rh(H)(Cl)[e]	55.1 −5.1	190 92			[59]
[^{i}Pr-PNP^{Me}]Ir(H)(Cl)	44.7				[57]
[^{i}Pr-PNP^{Me}]Ir(Me)(Cl)[e]	25.2				[57,59]
[^{i}Pr-PNP^{F}]Ir(Me)(Cl)[e]	24.4[g]				[59]
{Me[^{i}Pr-PNP^{Me}]*}Ir(H)(Cl) major	32.7 −32.4				[59]
{Me[^{i}Pr-PNP^{Me}]*}Ir(H)(Cl) minor	31.9 −40.3				[59]
{Me[^{i}Pr-PNP^{Me}]*}Ir(H)(Cl)			2.340(7)	2.288(3) 2.214(3)	[59]
{Me[^{i}Pr-PNP^{F}]*}Ir(H)(Cl) major	32.8 −31.6				[59]
{Me[^{i}Pr-PNP^{F}]*}Ir(H)(Cl) minor	32.0 −39.1				[59]
{Me[^{i}Pr-PNP^{Me}]}Ir(η^4-COD)$^+$[h]	12.8[f]				[59]
{Me[^{i}Pr-PNP^{F}]}Ir(η^4-COD)$^+$[h]	13.0[f]				[59]
[^{i}Pr-PNP^{C2}]Ir(Me)(Cl)[e]	20–40 (br)				[59]
{Me[^{i}Pr-PNP^{C2}]*}Ir(H)(Cl)[e]	38.3 −30.9				[59]
{[^{i}Pr-PNP^{C2}]CH$_2$}Ir(H)(Cl)[e]	28.9				[59]

Table 1 (*Continued*)

Compound	δ_P	$^1J_{PM}$	M—N distance (Å)	M—P distance (Å)	Reference
Group 10					
$\{[^i$Pr-NP]NiCl$\}_2$	32.5				[53]
[^{i}Pr-NP]NiCl(PMe_3)	47.3		1.923(3)	2.1556(10)	[53]
[^{i}Pr-NP]NiMe(PMe_3) major	35.6		1.939(3)	2.2009(12)	[53]
[^{i}Pr-NP]NiMe(PMe_3) minor	39.0				[53]
[^{i}Pr-NP]NiPh(PMe_3)	33.0		1.947(5)	2.149(2)	[53]
[^{i}Pr-NP]Ni(η^3-CH_2Ph)	36.2		1.908(4)	2.1231(15)	[53]
[Me-NP]Ni(η^3-CH_2Ph)	34.8		1.900(3)	2.1176(11)	[53]
[Ph-PNP]NiCl	18.8		1.895(3)	2.1737(9) 2.1879(8)	[23,54]
[Ph-PNP]NiBr	23.7		1.912(5)	2.1830(12) 2.1830(12)	[54]
[Ph-PNP]NiI	33.1				[54]
[^{i}Pr-PNP]NiCl	34.7		1.9030(17)	2.1884(6) 2.1913(6)	[54]
[Cy-PNP]NiCl	26.8				[54]
[^{i}Pr-PNP^{Me}]NiCl	34.2				[83]
[^{i}Pr-PNP^F]NiCl	33.6				[83]
[Ph-PNP]NiH[e]	33.2				[54]
[^{i}Pr-PNP]NiH	56.2				[54]
[Cy-PNP]NiH	47.0				[54]
[^{i}Pr-PNP^{Me}]NiH	56.2				[83]
[^{i}Pr-PNP^F]NiH	56.0				[83]
[Ph-PNP]NiMe	27.6		1.967(8)	2.1776(13) 2.1776(13)	[23]
[Ph-PNP]NiEt	26.4				[23]
[Ph-PNP]Ni(*n*-Bu)	27.1		1.966(2)	2.1655(8) 2.1811(8)	[23]
[Ph-PNP]Ni(*i*-Bu)	26.8				[23]
[Ph-PNP]Ni(CH_2SiMe_3)	23.9		1.966(5)	2.191(2) 2.154(2)	[23]
[Ph-PNP]NiPh	24.5				[23]
[^{i}Pr-PNP]NiMe	35.5		1.945(3)	2.1557(12) 2.1797(12)	[54]
[^{i}Pr-PNP]NiEt	32.1				[54]
[^{i}Pr-PNP]Ni(*n*-Bu)	32.5		1.953(3)	2.1576(9) 2.1966(9)	[54]
[Cy-PNP]NiMe	28.2		1.947(5)	2.1677(10) 2.1677(10)	[54]
[Cy-PNP]NiEt	24.6				[54]
[Cy-PNP]Ni(*n*-Bu)	25.1				[54]
[^{i}Pr-PNP^{Me}]NiMe	35.4				[83]
[^{i}Pr-PNP^F]NiMe	35.4				[83]
$\{[^i$Pr-NP]PdCl$\}_2$	57.8				[91]
[^{i}Pr-NP]PdCl(PCy_3)	52.2[b]		2.079(2)	2.2532(8)	[91]
[Ph-PNP]PdCl	29.8		2.056(11)	2.3010(18) 2.3010(18)	[88]
[Ph-PNP]PdOAc	29.1				[88]
[^{i}Pr-PNP]PdCl	48.5				[58]
[^{i}Pr-PNP]PdOAc	48.2				[58]
[^{i}Pr-PNP^{Me}]PdCl	48.2		2.026(2)	2.2913(9) 2.2913(9)	[56,58,83]
[^{i}Pr-PNP^{Me}]PdOAc	48.4				[56,58]
[^{i}Pr-PNP^F]PdCl	47.4				[58,83]

Table 1 (*Continued*)

Compound	δ_P	$^1J_{PM}$	M—N distance (Å)	M—P distance (Å)	Reference
[^{i}Pr-PNP^F]PdOAc	48.0		2.015(5)	2.2852(17) 2.2739(17)	[58]
[^{i}Pr-PNP^{Br}]PdCl	48.7				[58]
[^{i}Pr-PNP^{Br}]PdOAc	48.5				[58]
[^{i}Pr-PNP^{SiMe3}]PdCl	49.3				[58]
[^{i}Pr-PNP^{SiMe3}]PdOAc	48.7				[58]
[^{i}Pr-PNP^{Me}]PdH	59.8				[56,83]
[^{i}Pr-PNP^F]PdH	59.2		2.086(4)	2.2619(15) 2.2658(15)	[83]
[^{i}Pr-PNP^{Me}]PdMe	41.1				[83]
[^{i}Pr-PNP^F]PdMe	40.8		2.0938(15)	2.2914(3) 2.2914(3)	[83]
[^{i}Pr-PNP^{C2}]PdCl	49.4		2.068(4)	2.2643(13) 2.2504(13)	[59]
[Ph-PNP]PtCl	25.4	2751	2.024(6)	2.284(2) 2.270(2)	[89]
[Ph-PNP]PtMe	30.6	2983	2.09(2)	2.2737(18) 2.2737(18)	[89]
[Ph-PNP]PtOTf	27.8	2809			[89]
{[Ph-PNP]Pt(py)}OTf	28.9[b]	2660[b]	2.025(5)	2.2941(17) 2.2735(17)	[89]
{[Ph-PNP]Pt(NCMe)}OTf	29.0[i]	2555[i]			[89]
[Ph-PNP]PtPh	27.9	2967			[89]
[^{i}Pr-PNP^{Me}]PtCl	41.3	2666			[83]
[^{i}Pr-PNP^F]PtCl	40.7	2669			[83]
[^{i}Pr-PNP^{Me}]PtH	59.3	2781			[83]
[^{i}Pr-PNP^F]PtH	58.8	2792			[83]
[^{i}Pr-PNP^{Me}]PtMe	41.0	2840			[83]
[^{i}Pr-PNP^F]PtMe	40.9	2855			[83]
Group 11					
{[^{i}Bu-PNP]Cu}$_2$	−33.9		2.127(4) 2.191(4) 2.179(4) 2.219(4)	2.2173(13) 2.2339(13) 2.2235(13) 2.2241(13)	[55]
Group 12					
[^{i}Pr-NP]ZnMe	−27.3				[28]
[^{i}Pr-NP]ZnEt	−27.2		1.911(4)	2.4450(14)	[28]
[^{i}Pr-NP]$_2$Zn	−22.9		1.971(5) 1.974(5)	2.4545(19) 2.4387(19)	[28]
Group 13					
[Me-NP]AlCl$_2$	−36.1				[52]
[^{i}Pr-NP]AlCl$_2$	−34.4				[52]
[Me-NP]AlCl$_2$(THF)	−34.8		1.870(4)	2.5882(19)	[52]
[^{i}Pr-NP]AlCl$_2$(THF)	−33.7				[52]
[Me-NP]AlMe$_2$	−24.1				[52]
[Me-NP]AlEt$_2$	−24.0		1.894(8)	2.456(4)	[52]
[^{i}Pr-NP]AlMe$_2$	−21.6		1.894(6)	2.477(3)	[52]
[^{i}Pr-NP]AlEt$_2$	−21.4				[52]
[Me-NP]Al(CH$_2$SiMe$_3$)$_2$	−24.2				[52]

[a] The data summarized correspond to the diarylamido phosphine ligands only. Unless otherwise noted, all NMR spectra were recorded in C_6D_6 at room temperature, chemical shifts in ppm, coupling constants in Hz.
[b] Spectra were recorded in $CDCl_3$.
[c] Spectra were recorded in toluene-d_8.
[d] Spectra were recorded at −20 °C.
[e] Spectroscopically observed, not isolated.
[f] Spectra were recorded in CD_2Cl_2.
[g] Spectra were recorded in $PhCF_3$.
[h] The anions are a mixture of Cl^- and $[(COD)IrCl_2]^-$.
[i] Spectra were recorded in THF.

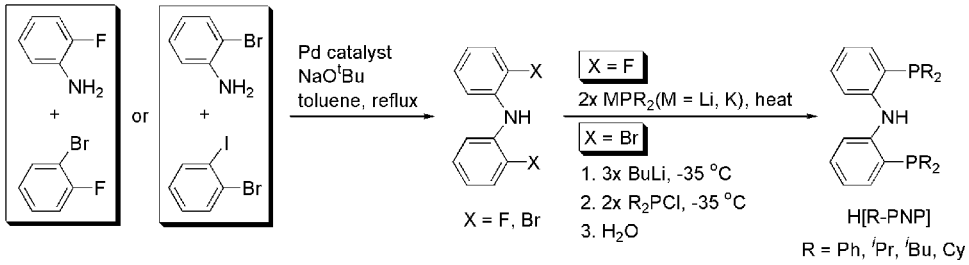

Scheme 2.

2.2. Tridentate amido diphosphine ligands

2.2.1. Protonated precursors

Following the same strategy as that for the preparation of H[NP], a number of diphosphino-diarylamine derivatives (H[PNP]) are readily accessible. Scheme 2 summarizes two attractive protocols for the preparation of H[N(*o*-C$_6$H$_4$PR$_2$)$_2$] (H[R-PNP]; R = Ph, ^{i}Pr, ^{i}Bu, Cy). The desired compounds are all available in two steps from commercially available starting materials. Thus, both *o*-fluoro-substituted [23] and *o*-bromo-substituted [54] biphenyl amines were prepared quantitatively from the palladium catalyzed aryl amination reactions of either 2-fluoroaniline with 2-bromofluorobenzene or 2-bromoaniline with 2-bromoiodobenzene. Subsequent replacement of the fluorine atoms in di(2-fluorophenyl)amine with diphenyl- or diisobutylphosphide in ethereal solutions produced H[Ph-PNP] [23] and H[^{i}Bu-PNP] [55], respectively. Sequential addition of *n*-BuLi and R$_2$PCl (R = Ph, ^{i}Pr, Cy) to a diethyl ether solution of di(2-bromophenyl)amine at −35 °C generated the corresponding H[R-PNP] [54] after anaerobic aqueous workup. It is interesting to note that [Cy-PNP]Li(OEt$_2$) may be conveniently isolated as a crystalline solid prior to aqueous workup. Compound (2-^{i}Pr$_2$P-4-MeC$_6$H$_3$)$_2$NH (H[^{i}Pr-PNP^{Me}]) that contains a tolylene backbone was prepared analogously [56].

Solution NMR spectroscopic data are indicative of C_{2v} symmetry for these molecules. The NH proton in these compounds appears as one triplet resonance with J_{HP} of ca. 8 Hz due to the internuclear coupling with the two chemically equivalent phosphorus atoms. Compound H[Ph-PNP] was characterized by X-ray crystallography [23].

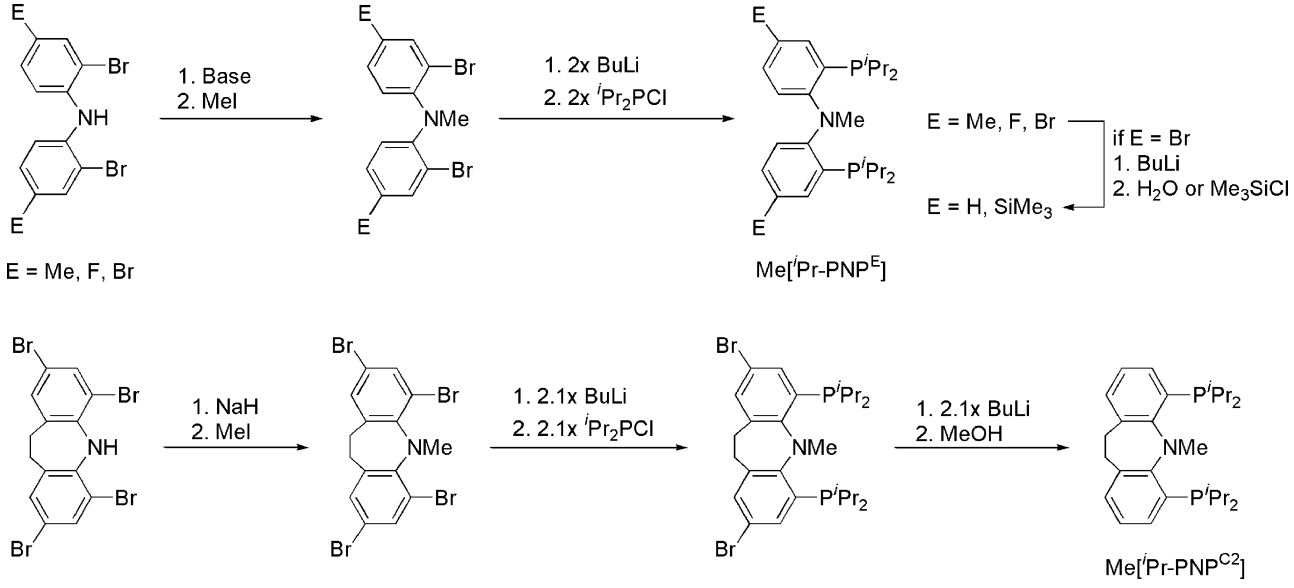

Scheme 3.

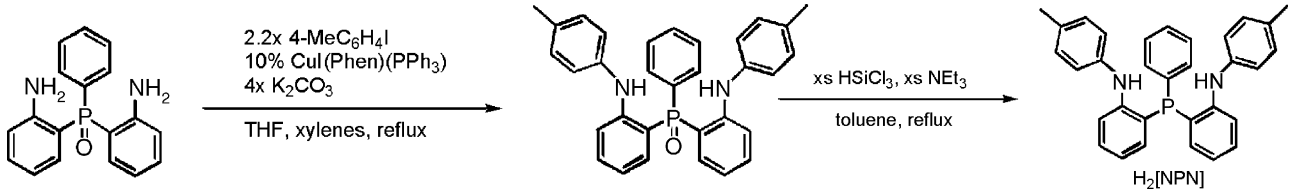

Scheme 4.

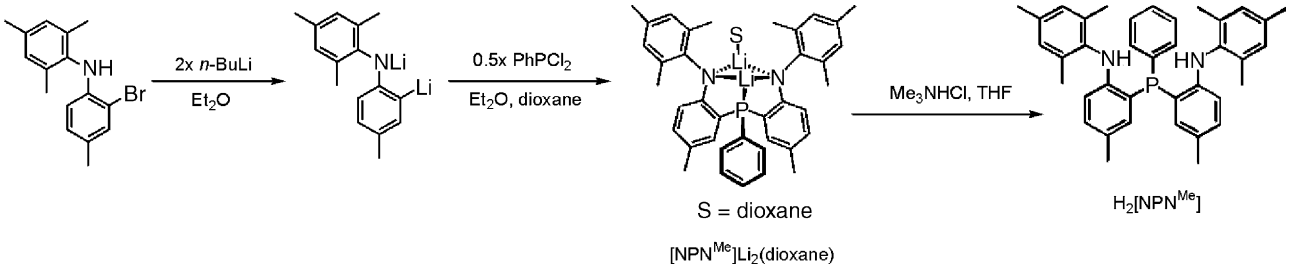

Scheme 5.

2.2.2. *Methylated precursors*

N-Methylated diphosphino-diarylamine compounds were also prepared. Most incorporate substituted aryl bridges to connect the nitrogen and phosphorus donors. As shown in Scheme 3, methylation at the diarylamine nitrogen atom was generally performed prior to phosphanylation [57–59]. The N–Me protons in these molecules were all observed as a singlet resonance in the ^{1}H NMR spectroscopy. The fluorinated compound (2-^{i}Pr$_2$P-4-FC$_6$H$_3$)$_2$NMe (Me[^{i}Pr-PNP^F]) was characterized crystallographically [59].

2.3. *Tridentate diamido phosphine ligands*

The reaction of 2,2′-diaminotriphenylphosphine oxide with 4-iodotoluene catalyzed by CuI(phen)(PPh$_3$) produced [(4-MeC$_6$H$_4$)NH(2-C$_6$H$_4$)]$_2$PhP=O, which was then reduced under standard conditions to give the desired [(4-MeC$_6$H$_4$)NH(2-C$_6$H$_4$)]$_2$PPh (H$_2$[NPN], Scheme 4) [60]. This protocol, however, is perhaps not favorable for a multigram scale reaction due, at least in part, to the formation of a side product [(4-MeC$_6$H$_4$)$_2$N(2-C$_6$H$_4$)][(4-MeC$_6$H$_4$)NH(2-C$_6$H$_4$)]PhP=O arising from arylation of [(4-MeC$_6$H$_4$)NH(2-C$_6$H$_4$)]$_2$PhP=O in the copper catalyzed reaction. Extensive chromatography was thus required for the purification of [(4-MeC$_6$H$_4$)NH(2-C$_6$H$_4$)]$_2$PhP=O prior to reduction.

Scheme 5 summarizes an alternative route for the preparation of the desired compounds. Sequential addition of *n*-BuLi and PhPCl$_2$ to a diethyl ether solution of (2-Br-4-MeC$_6$H$_3$)(2,4,6-Me$_3$C$_6$H$_2$)NH produced the solvated lithium complex [(2,4,6-Me$_3$C$_6$H$_2$)NLi-2-(5-MeC$_6$H$_3$)]$_2$PPh (Li$_2$[NPN^{Me}]) [60]. The lithium compound has been structurally characterized as a bis(tetrahydrofuran) adduct. Protonation of the lithium compound with trimethylammonium chloride in THF generated [(2,4,6-Me$_3$C$_6$H$_2$)NH-2-(5-MeC$_6$H$_3$)]$_2$PPh (H$_2$[NPN^{Me}]). Similar to that found for H[^{i}Pr-NP] [28,53], the *N*-mesityl bond rotation is hindered for H$_2$[NPN^{Me}] due to the steric size of the

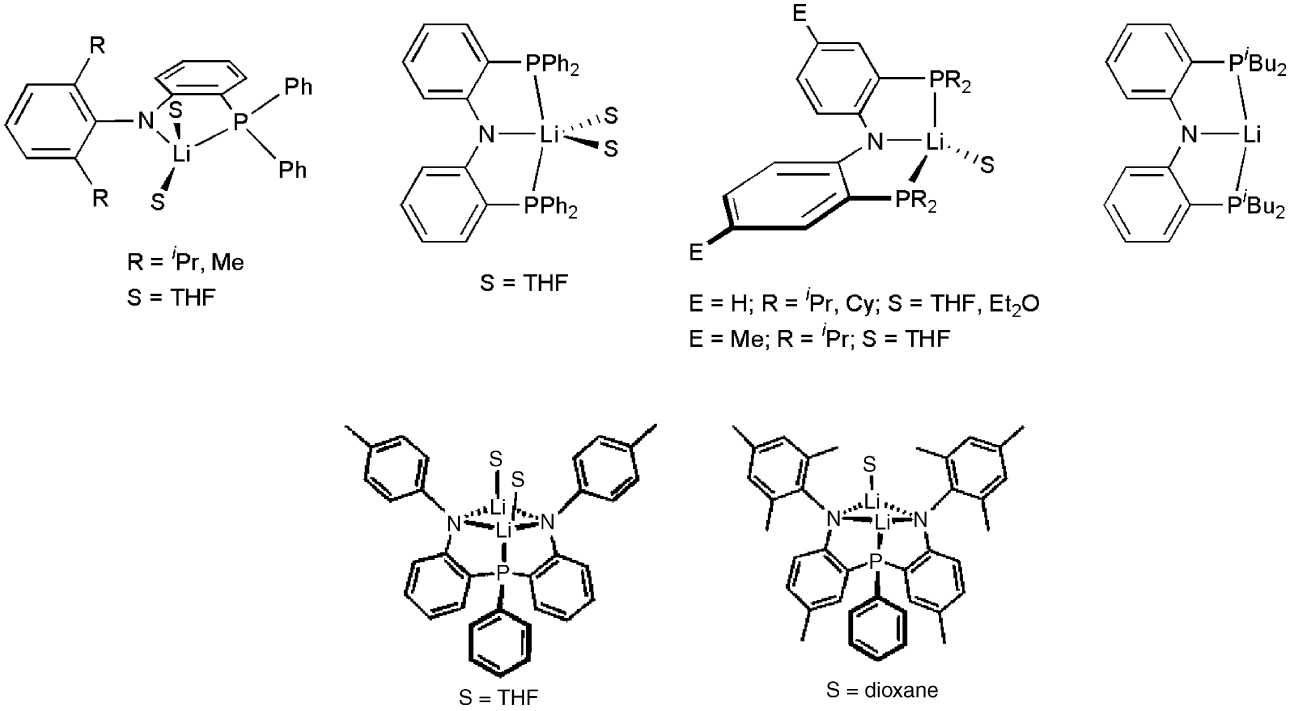

Fig. 4. Lithium complexes of diarylamido phosphine ligands.

mesityl group. The rotation barrier $\Delta G^{\neq}_{rot}$ about the *N*-mesityl bond in this molecule was calculated to be 15.5 ± 0.3 kcal mol^{-1} [60].

3. Metal complexes

3.1. Group 1: lithium

Lithium amides are convenient starting materials for metathetical reactions with main-group and transition metal halides. As a result, the preparation of lithium complexes of these chelating amido phosphine ligands has become typical. Lithiation of the protonated ligand precursors was generally performed with the employment of *n*-BuLi, usually in ethereal solutions, to produce the corresponding lithium complexes as solvent adducts. The number of coordinated solvent molecules varies (Fig. 4), depending on the electronic and steric characteristics of the amido phosphine ligands.

The coordination chemistry of these amido phosphine ligands with respect to lithium has been assessed by ^{31}P and ^{7}Li ($I = 3/2$, natural abundance 92.6%) NMR spectroscopy. The number of coordinated solvent molecules could be readily determined by ^{1}H NMR spectroscopy. As summarized in Table 1, the phosphorus donors generally exhibit a downfield shift for the monoanionic [NP]$^{-}$ or [PNP]$^{-}$ ligands upon lithiation, whereas those in dianionic [NPN]$^{2-}$ are shifted relatively upfield as compared to the corresponding ligand precursors. The $^{1}J_{PLi}$ values of triaryl phosphine complexes (34–41 Hz) [23,53,54,60] are consistently lower than those of alkyl-substituted counterparts (46–61 Hz) [54,61]. The distinct values of $^{1}J_{PLi}$ is perhaps a consequence of diverse electronic properties of the substituents at the phosphorus donors or a result of different electrophilicity of the lithium center due to various amount of coordinate ethereal molecules. Interestingly, the phosphorus donor in [NPN^{Me}]Li$_2$(dioxane) [60] appears as a quartet resonance at -35.2 ppm in the ^{31}P{^{1}H} NMR spectroscopy and the lithium atoms exhibit a doublet at -0.1 ppm and a singlet at -2.0 ppm, consistent with one of the lithium atoms is not bound to the phosphorus donor. The X-ray structure of [NPN^{Me}]Li$_2$(THF)$_2$ is shown in Fig. 5.

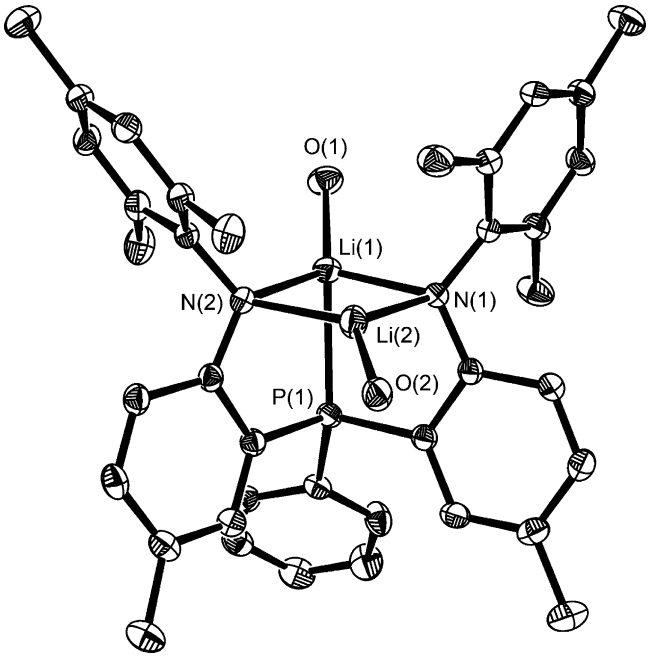

Fig. 5. Molecular structure of [NPN^{Me}]Li$_2$(THF)$_2$ established from an X-ray study [60]. All carbon atoms in coordinated THF are omitted for clarity.

Several lithium complexes have been characterized by X-ray crystallography. The solid-state structures are generally in good agreement with the solution structures determined by NMR spectroscopy. The Li–N and Li–P bond distances are summarized in Table 1. Although these parameters are all well within the expected values and consistent with each other, it is interesting to note that the coordination modes of the chelating amido phosphine ligands may depend on the substituents at the donor atoms, such as those found in [Ph-PNP]Li(THF)$_2$ (meridional) [23] and [Cy-PNP]Li(OEt$_2$) (facial) [54] as evidenced by the dihedral angles of 174.6° and 143.1°, respectively, for the two N–Li–P planes. Fig. 6 illustrates the molecular structures of [Ph-PNP]Li(THF)$_2$ and [Cy-PNP]Li(OEt$_2$).

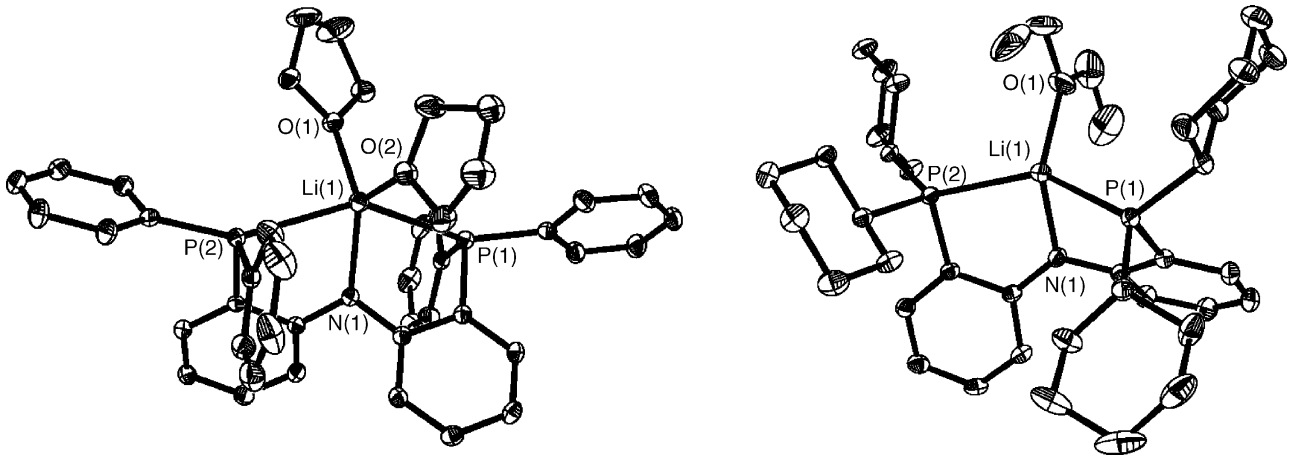

Fig. 6. Molecular structures of [Ph-PNP]Li(THF)$_2$ (left) and [Cy-PNP]Li(OEt$_2$) (right) established from X-ray studies [23,54].

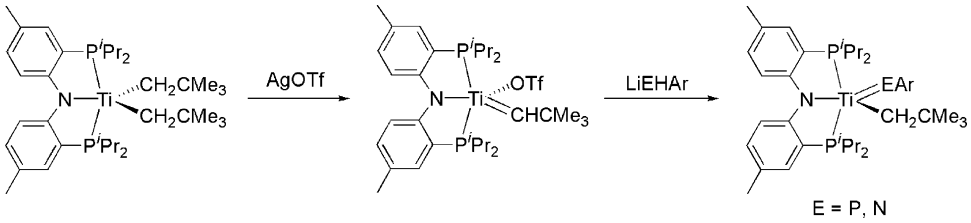

Scheme 6.

3.2. Group 4

3.2.1. Titanium

The only report regarding titanium to date involves [^{i}Pr-PNP^{Me}]$^-$ [62]. An attractive entry into the titanium chemistry appears to be the one-pot reaction of [^{i}Pr-PNP^{Me}]Li [61] with $TiCl_3(THF)_3$ in toluene at −35 °C followed by alkylation with two equiv of neopentyllithium to give the dineopentyl complex [^{i}Pr-PNP^{Me}]Ti(CH_2CMe_3)$_2$. The use of Ti(III) precursors instead of Ti(IV) avoids the facile reduction of Ti(IV) upon alkylation. One electron oxidation of [^{i}Pr-PNP^{Me}]Ti(CH_2CMe_3)$_2$ with AgOTf in pentane at −35 °C produced a terminal neopentylidene complex [^{i}Pr-PNP^{Me}]Ti(=$CHCMe_3$)(OTf) (Scheme 6), presumably arising from α-abstraction [63] of the putative [^{i}Pr-PNP^{Me}]Ti(CH_2CMe_3)$_2$(OTf). The $^{31}P\{^1H\}$ NMR spectrum of [^{i}Pr-PNP^{Me}]Ti(=$CHCMe_3$)(OTf) displays two doublet resonances centered at 33.6 and 24.2 ppm with $^2J_{pp}$ of 55 Hz. The Ti=CH_α appears at 8.42 ppm in the ^{1}H NMR spectrum and the diagnostic Ti=C_α atom at 301 ppm in the ^{13}C NMR spectrum with a low $^1J_{CH}$ of 103 Hz, indicative of an α-agostic interaction [41,64] being present in this molecule. These results are further supported by an X-ray study of [^{i}Pr-PNP^{Me}]Ti(=$CHCMe_3$)(OTf) (Fig. 7), which reveals a short Ti=C distance (1.881(7) Å), a wide Ti=C_α–C_β angle (157.6(6)°), and a short Ti–H_α distance (2.09(6) Å) in a distorted trigonal bipyramidal geometry, in which the two phosphorus donors are virtually trans to each other.

Addition of one equiv of LiPHAr (Ar = 2,4,6-$C_6H_2{}^iPr_3$) or LiNHAr (Ar = 2,6-$C_6H_3{}^iPr_2$) to a diethyl ether solution of [^{i}Pr-PNP^{Me}]Ti(=$CHCMe_3$)(OTf) at −35 °C produced the corresponding phosphinidene and imide complexes [^{i}Pr-PNP^{Me}]Ti(=EAr)(CH_2CMe_3) (E = P, N). The formation of [^{i}Pr-PNP^{Me}]Ti(=EAr)(CH_2CMe_3) was proposed to proceed from the presumed [^{i}Pr-PNP^{Me}]Ti(=$CHCMe_3$)(EHAr) followed by α-hydrogen migration from the phosphide or anilide donor to the nucleophilic Ti=C_α atom. The signal found at 237 ppm in the $^{31}P\{^1H\}$ NMR spectrum is indicative of a linear phophinidene structure. The Ti=P distance of 2.2066(4) Å is significantly short as compared to the dative Ti–P of ca. 2.60 Å in [^{i}Pr-PNP^{Me}]Ti(=PAr)(CH_2CMe_3) (Fig. 7). In contrast to the titanium phosphinidene complexes [Nacnac]Ti(=PAr)(CH_2CMe_3) (Ar = Cy, 2,4,6-$C_6H_2{}^iPr_3$, 2,4,6-$C_6H_2{}^tBu_3$) which undergo further undesired reactions involving the β-diketiminate ligand ([Nacnac] = ArNC(Me)CHC(Me)NAr; Ar = 2,6-$C_6H_3{}^iPr_2$) [65], [^{i}Pr-PNP^{Me}]Ti(=PAr)(CH_2CMe_3) is kinetically and thermally stable, a result that is ascribed to the robustness of the diarylamido phosphine ligand.

3.2.2. Zirconium

Zirconium(IV) complexes of bidentate amido phosphine ligands have been prepared [66]. Both mono- and bis-ligated complexes could be isolated effectively, depending strictly on the stoichiometry and steric size of the amido phosphine ligands employed (Scheme 7). Thus, addition of one equiv of [^{i}Pr-NP]Li$(THF)_2$ to $ZrCl_4(THF)_2$ in toluene at −35 °C led to the formation of [^{i}Pr-NP]$ZrCl_3$(THF) in 72% yield, whereas the reaction of $ZrCl_4(THF)_2$ with two equiv of sterically less demanding [Me-NP]Li$(THF)_2$ produced [Me-NP]$_2ZrCl_2$ in 92% yield.

The solid-state structures of both [^{i}Pr-NP]$ZrCl_3$(THF) and [Me-NP]$_2ZrCl_2$ were determined by X-ray crystallography,

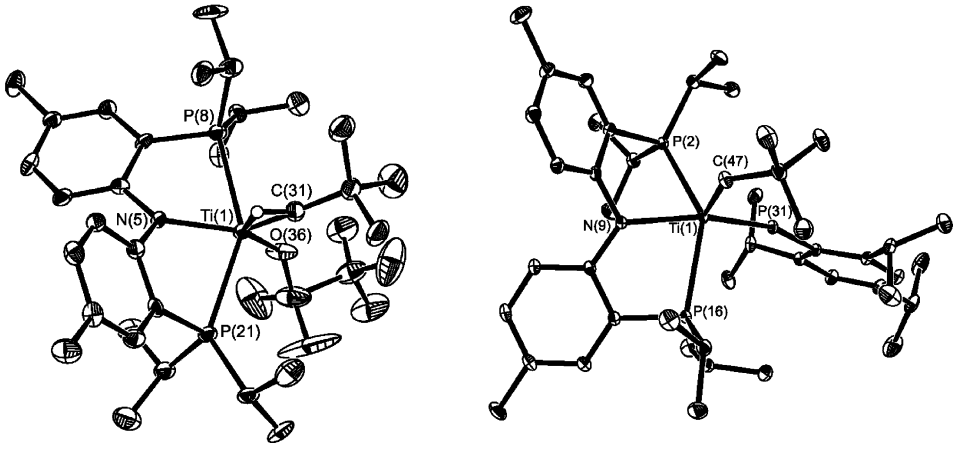

Fig. 7. Molecular structures of [^{i}Pr-PNP^{Me}]Ti(=$CHCMe_3$)(OTf) (left) and [^{i}Pr-PNP^{Me}]Ti(=PAr)(CH_2CMe_3) (right, Ar = 2,4,6-$C_6H_2{}^iPr_3$) established from X-ray studies [62].

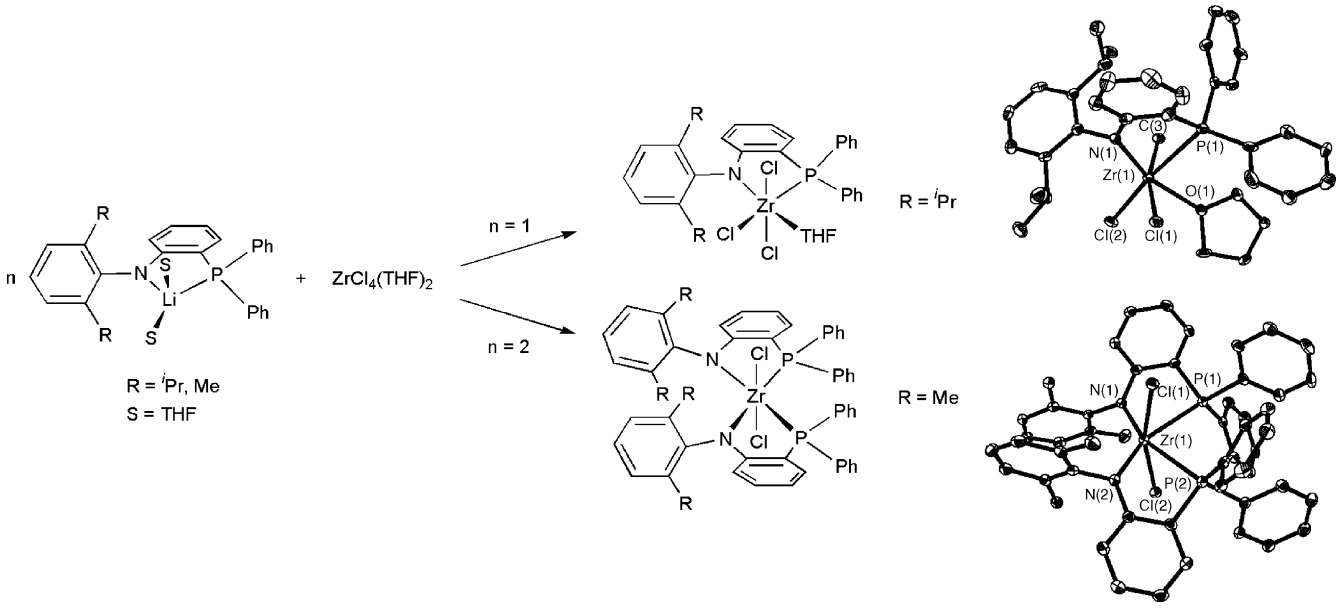

Scheme 7.

which reveals a distorted octahedral geometry for these molecules and severe displacement of zirconium from the corresponding mean N–phenylene–P planes. The deviation of the zirconium center is likely a consequence of either the relatively large size of zirconium with respect to the rigid amido phosphine ligands or the steric repulsion arising from the bulky substituents at the nitrogen and phosphorus donor atoms. These results are in accord with the solution NMR data. In particular, the isopropylmethyl groups in [^{i}Pr-NP]$ZrCl_3$(THF) are diastereotopic, due to restricted rotation of the *N*-aryl bond. The phosphorus donors in [^{i}Pr-NP]$ZrCl_3$(THF) and [Me-NP]$_2ZrCl_2$ are observed as a singlet resonance at 1.95 and 12.28 ppm, respectively, which is shifted relatively downfield from those of H[^{i}Pr-NP] and [^{i}Pr-NP]Li(THF)$_2$, consistent with phosphorus coordination to the electron-deficient group 4 metals in solution.

The preparation of zirconium(IV) complexes containing a tridentate amido diphosphine ligand was also reported [61]. Treatment of [^{i}Pr-PNP^{Me}]Li(THF) with $ZrCl_4(OEt_2)_2$ in toluene at −35 °C produced [^{i}Pr-PNP^{Me}]$ZrCl_3$ in 85% yield. Alkylation of the chloride complex with Grignard reagents generated the corresponding [^{i}Pr-PNP^{Me}]Zr(CH_2R)$_3$ (R = H, Ph, *p*-tolyl). The trimethyl complex was characterized crystallographically. Interestingly, α-abstraction occurs for the tribenzyl derivatives at ambient temperature to give benzylidene complexes [^{i}Pr-PNP^{Me}]Zr(=CHR)(CH_2R) (Scheme 8). The diagnostic Zr=C_α signal appears at ca. 230 ppm with $^1J_{CH}$ of 92 Hz, consistent with an α-agostic interaction [64]. The Zr=CH_α displays a signal at ca. 7.3 ppm and the two phosphorus donors resonate at ca. 28 and 27 ppm with $^2J_{pp}$ of 59 Hz. A kinetic study revealed a first-order rate law for the α-abstraction reaction shown in Scheme 8. The activation parameters for this process at temperatures from 20 to 53 °C were determined: $\Delta H^{\neq} = 19 \pm 1$ kcal mol^{-1}, $\Delta S^{\neq} = -14 \pm 3$ cal mol^{-1} K^{-1}, and $\Delta G^{\neq}_{298} = 23 \pm 2$ kcal mol^{-1}. These results, particular the $\Delta S^{\neq}$ value, likely reflect the significance of the rigidity imposed by the diarylamido diphosphine ligand as compared to the corresponding parameters (e.g., $\Delta S^{\neq} = -22 \pm 5$ cal mol^{-1} K^{-1}) calculated from that producing the first zirconium alkylidene complex [P_2Cp]Zr(=CHPh)Cl ([P_2Cp] = η^5-C_5H_3-1,3-($SiMe_2CH_2P^iPr_2$)$_2$) [67–69] by thermolysis of [P_2Cp]Zr(CH_2Ph)$_2$Cl, which contains only one rather than two coordinated phosphine arms in the ground state. No crystallographic data is available to date for zirconium alkylidene complexes supported by diarylamido phosphine ligands.

Unlike those of monoanionic [NP]$^-$ and [PNP]$^-$, an effective entry for the preparation of zirconium(IV) complexes of dianionic [NPN]$^{2-}$ appears to involve the protonated ligand precursors [60]. Protonolysis of Zr(NMe_2)$_4$ with H_2[NPN^{Me}] in toluene at room temperature produced [NPN^{Me}]Zr(NMe_2)$_2$ in 90% yield (Scheme 9). Subsequent reaction of [NPN^{Me}]Zr(NMe_2)$_2$ with an excess amount of trimethylsilylchloride generated [NPN^{Me}]$ZrCl_2$, which was reacted with MeMgCl in diethyl ether at −35 °C to give [NPN^{Me}]$ZrMe_2$. The solution NMR spectroscopic data of these complexes and the X-ray structure of [NPN^{Me}]$ZrCl_2$ are all consistent with a trigonal bipyramidal geometry for zirconium with the diamido phosphine ligand being in a facial coordination mode. The *ortho*-methyl groups in the *N*-mesityl substituents are chemically inequivalent at room temperature, indicating a

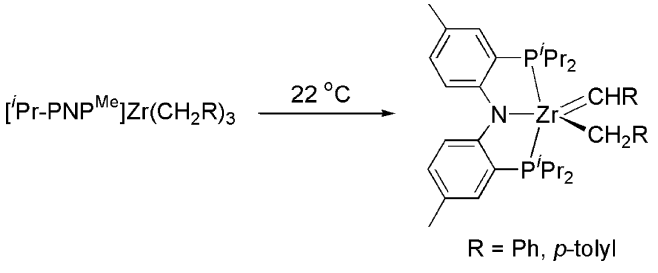

Scheme 8.

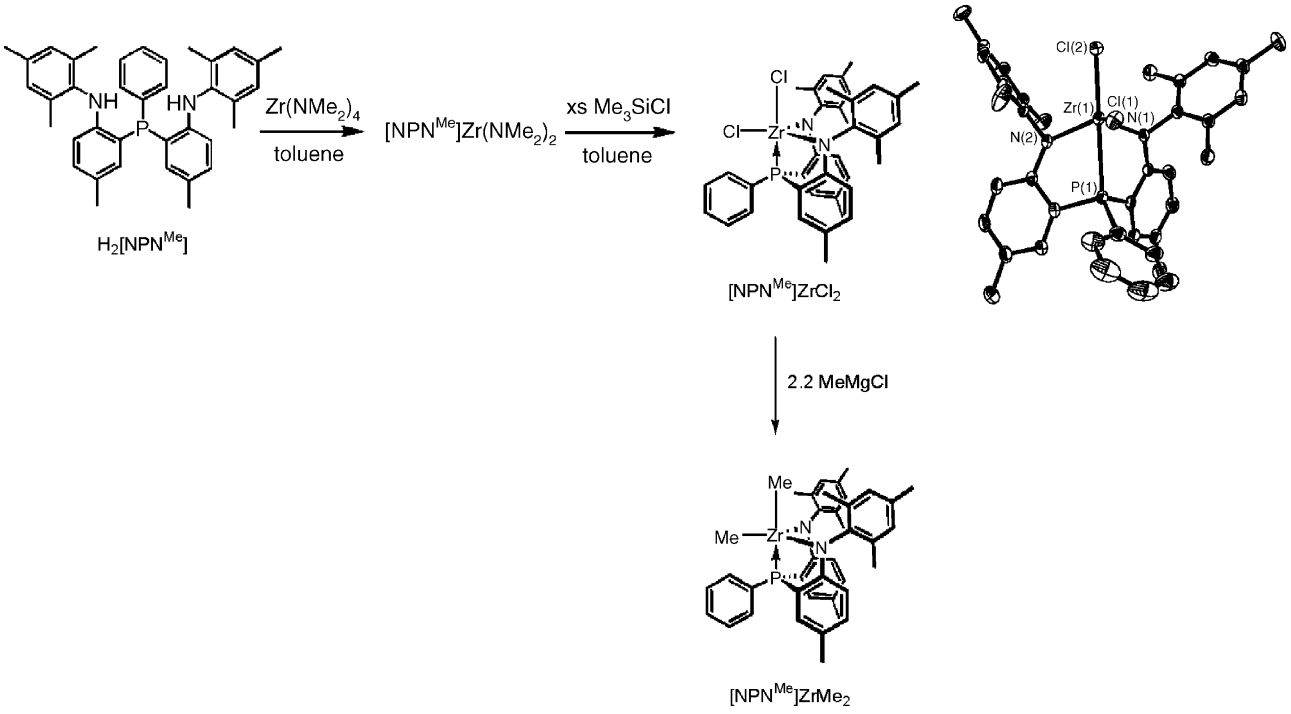

Scheme 9.

slow rotation about the N–Ar bonds for these molecules on the NMR time scale, due possibly to the steric reason.

3.2.3. Hafnium

The only isolated hafnium complexes reported to date are [^{i}Pr-NP]$HfCl_3$(THF) and [Me-NP]$_2HfCl_2$ [66], prepared from the reactions analogous to those illustrated in Scheme 7. These hafnium(IV) complexes are isostructural with the corresponding zirconium counterparts, given the comparable parameters obtained for these compounds from solution NMR spectroscopy and X-ray crystallography.

3.3. Group 8: ruthenium

Decarbonylation of acetone and carbonate was found to proceed at a ruthenium center supported by a diarylamido diphosphine ligand [70]. Thermolysis of [^{i}Pr-PNP^{Me}]Ru(H)(H_2), prepared from the reaction of H[^{i}Pr-PNP^{Me}] with [(COD)$RuCl_2$]$_n$ followed by reduction with $NaBH_4$, in the presence of acetone led to the formation of [^{i}Pr-PNP^{Me}]Ru(H)(CO) (Scheme 10), a result that was proposed to arise from sequential cleavage of the acetone C–C bond and decarbonylation of the presumed acyl intermediate complex. Alternatively, the reaction of H[^{i}Pr-PNP^{Me}] with [(COD)$RuCl_2$]$_n$ in the presence of $K_2{}^{13}CO_3$ in isopropanol at 80 °C generated ^{13}C-enriched (75%) decarbonylation product. Controlled experiments confirmed that both carbonate and secondary alcohols, e.g., isopropanol, can be decarbonylated. An X-ray study of [^{i}Pr-PNP^{Me}]Ru(H)(CO) revealed a roughly square pyramidal geometry for the ruthenium atom with the hydride ligand occupying the apical position (Fig. 8). The geometry of [^{i}Pr-PNP^{Me}]Ru(H)(H_2) was assessed by DFT optimization [70,71].

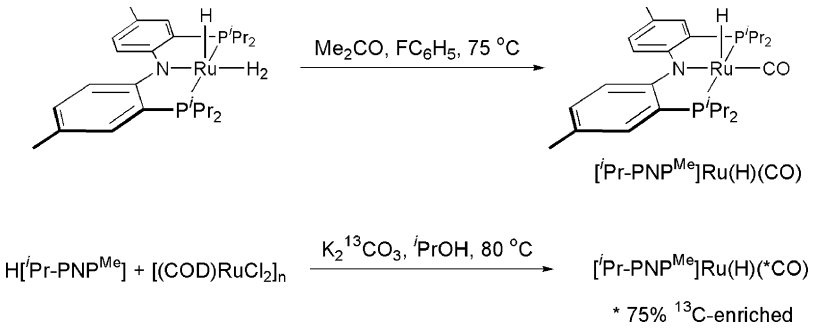

Scheme 10.

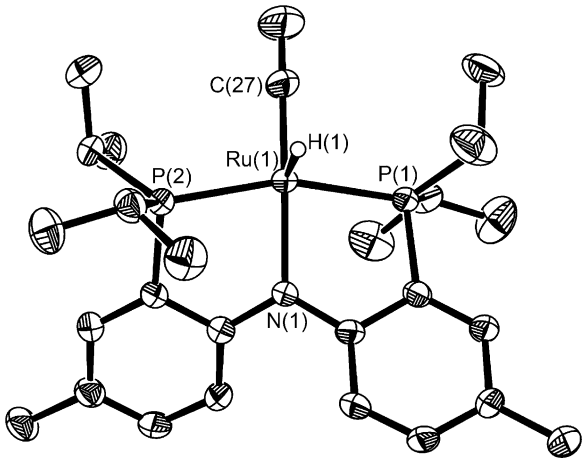

Fig. 8. Molecular structure of [^{i}Pr-PNP^{Me}]Ru(H)(CO) established from an X-ray study [70].

3.4. Group 9

3.4.1. Rhodium

The reaction of H[Ph-PNP] with $[(COE)_2RhCl]_2$ (COE = cyclooctene) in THF produced a five-coordinate rhodium(III) hydride complex [Ph-PNP]Rh(H)(Cl) (Scheme 11) [29]. The formation of [Ph-PNP]Rh(H)(Cl) represents the first example of N–H bond oxidative addition to a metal supported by a diarylamido phosphine ligand. The diagnostic upfield chemical shift of −21.8 ppm observed for Rh–H ($^{1}J_{RhH}$ = 30 Hz, $^{2}J_{PH}$ = 11 Hz) in the ^{1}H NMR spectrum is typical for d^6 metals that adopt a square pyramidal geometry in which the hydride ligand occupies the apical position [72–75]. The preference of the hydride ligand for the apical position is consistent with its high trans influence. Analogous reactions involving H[^{i}Pr-PNP^{Me}] were also reported to produce [^{i}Pr-PNP^{Me}]M(H)(Cl) (M = Rh, Ir) [57], accompanied by the isomerization of 1,5-COD (COD = cyclooctadiene) to 1,3-COD.

In situ lithiation of H[Ph-PNP] followed by reaction with $[(COE)_2RhCl]_2$ in toluene at room temperature generated a square-planar η^2-COE adduct [Ph-PNP]Rh(COE) [29]. The COE ligand was readily replaced by CO to give [Ph-PNP]Rh(CO). Alternative, [Ph-PNP]Rh(CO) could be prepared from the reaction of H[Ph-PNP] with $RhCl_3$ hydrate to give $\{H[Ph\text{-}PNP]\}Rh(\mu\text{-}Cl)_2(RhCl_2)$, which was subsequently reduced with sodium amalgam in the presence of CO. The structural parameters of [Ph-PNP]Rh(CO) obtained from an X-ray study were found to be generally in line with those predicted by density functional calculations [29]. The theoretical calculations also suggested that both amido nitrogen and Rh are negatively charged and no interaction between the amido pπ orbital and the Rh dπ orbital (or d_{yz} if the y axis is parallel to the Rh–N bond and the z axis perpendicular to the coordination plane of the amido diphosphine ligand). As a result, π back-bonding from Rh to CO is significant as evidenced by the CO stretching frequency of 1960 cm^{-1} [29].

Bond activation of the NMe group in *N*-methylated diarylamido diphosphine ligands was investigated. It was found that both N–C and C–H bonds in NMe can be activated by Rh(I) [57,59], depending on the ligands employed, to

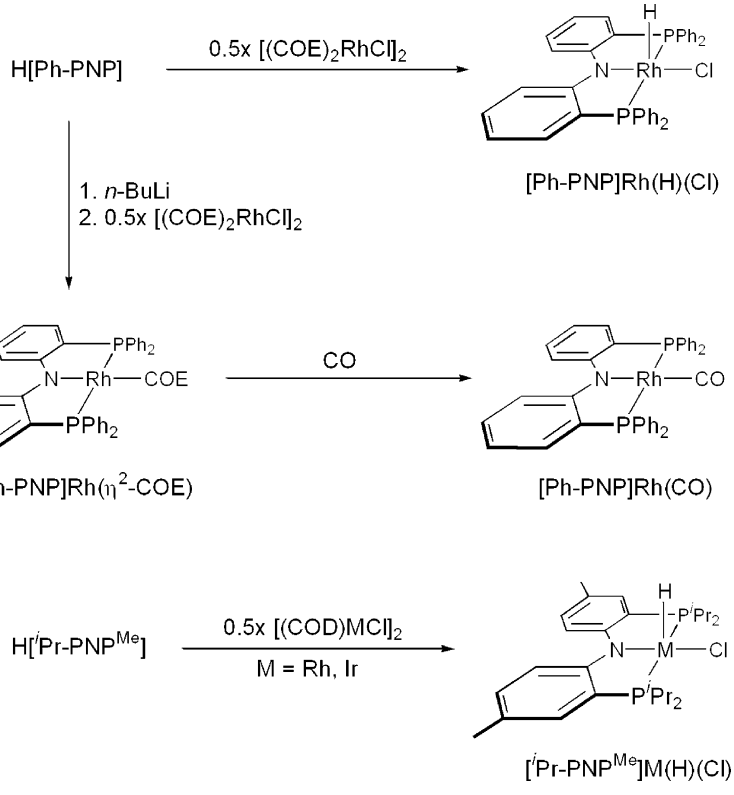

Scheme 11.

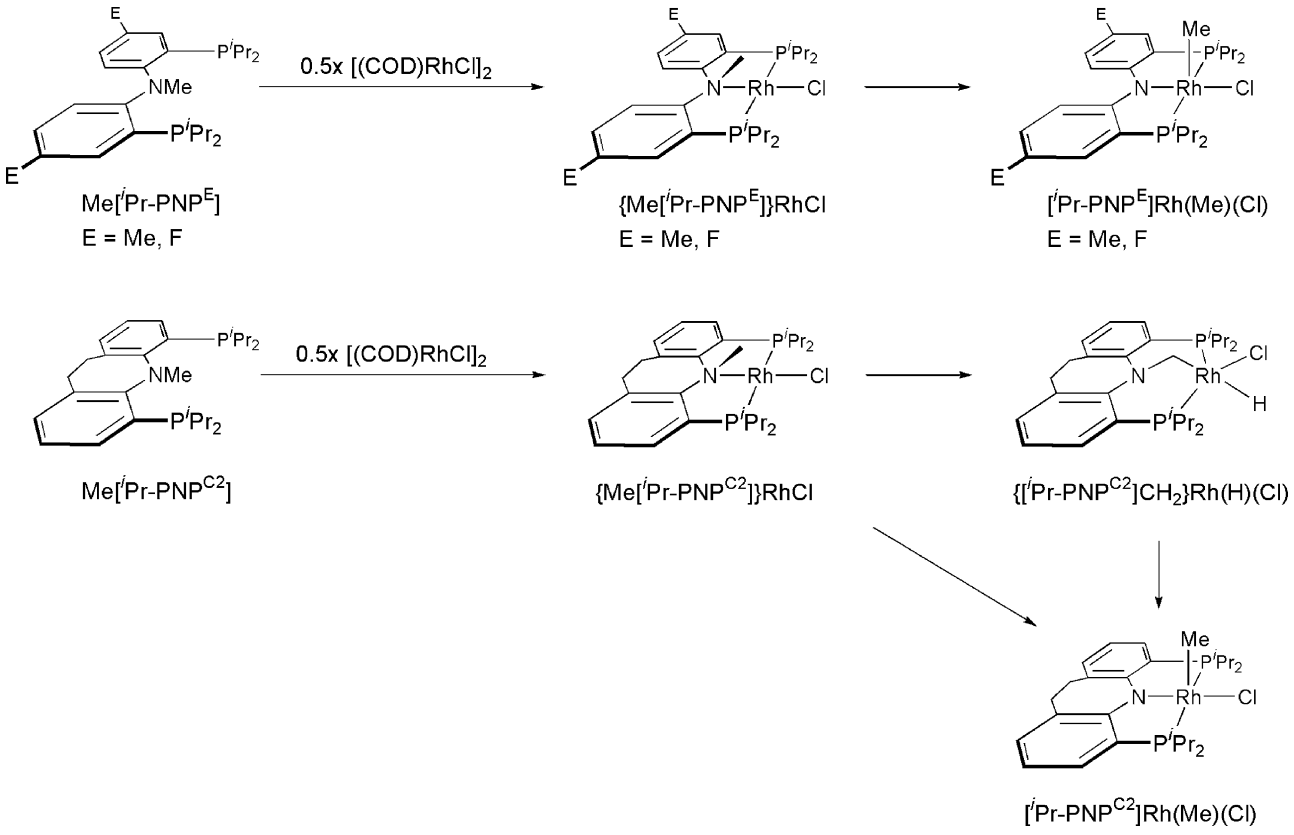

Scheme 12.

generate rhodium(III) complexes containing an either amido diphosphine ([^{i}Pr-PNP^E]$^-$ or [^{i}Pr-PNP^{C2}]$^-$; E = Me, F) or alkyl diphosphine ({[^{i}Pr-PNP^{C2}]CH$_2$}$^-$) ligand (Scheme 12). The reactions of Me[^{i}Pr-PNP^E] (E = Me, F) with [(COD)RhCl]$_2$ in diethyl ether at room temperature produced {Me[^{i}Pr-PNP^E]}RhCl, a product arising from the substitution of COD with the *N*-methylated diarylamido diphosphine ligand. These Rh(I) complexes subsequently transformed into [^{i}Pr-PNP^E]Rh(Me)(Cl) intramolecularly either in solution or in the solid state at temperatures ranging from 22 to 70 °C. The thermal transformation in the solid state (from crystal to crystal) is phenomenal. The activation parameters for the transformation of {Me[^{i}Pr-PNP^{Me}]}RhCl in C_6D_6 at temperatures from 25 to 62 °C were determined: $\Delta H^{\neq} = 23.5 \pm 0.9$ kcal mol^{-1}, $\Delta S^{\neq} = -2 \pm 3$ kcal mol^{-1} K^{-1}, and $\Delta G^{\neq}_{298} = 24.0 \pm 1.8$ kcal mol^{-1} [57]. The $\Delta S^{\neq}$ value obtained implies little change in order in the transition state, consistent with a direct 1,2-migration of Me from

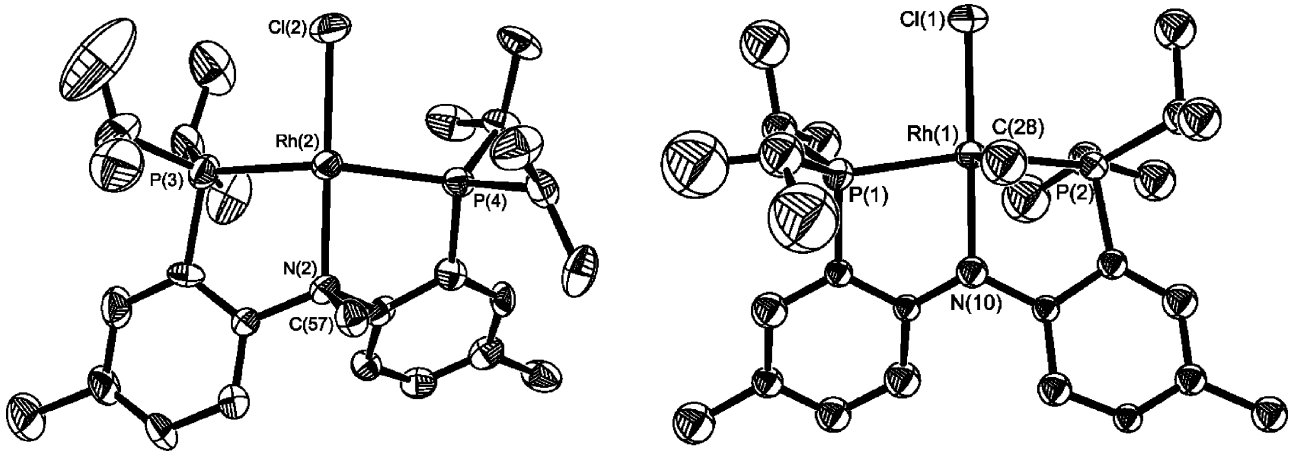

Fig. 9. Molecular structures of {Me[^{i}Pr-PNP^{Me}]}RhCl (left) and [^{i}Pr-PNP^{Me}]Rh(Me)(Cl) (right) established from X-ray studies [57].

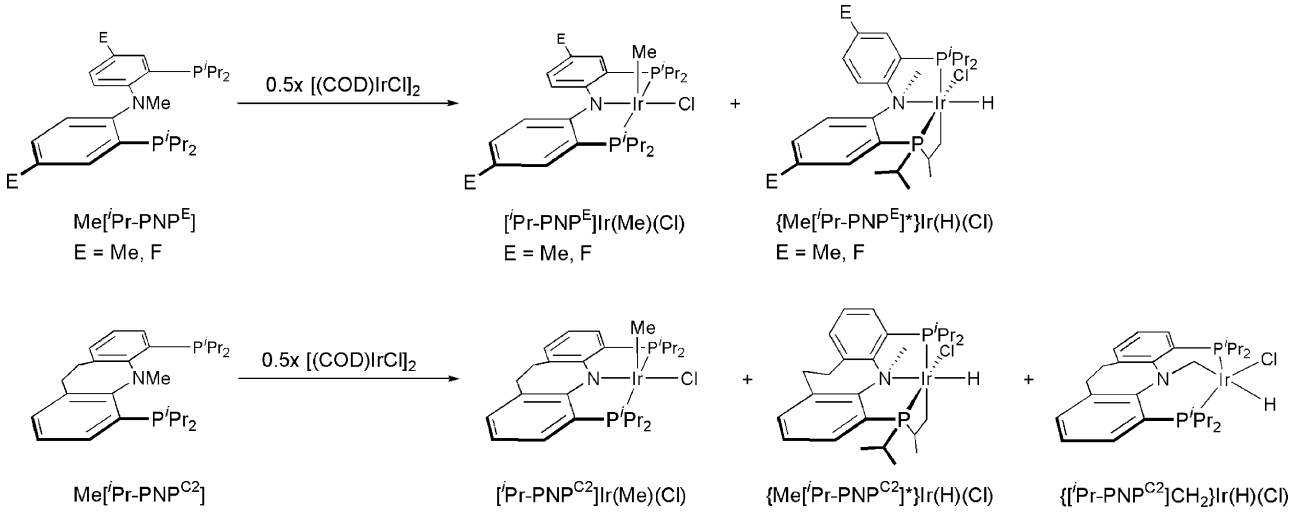

Scheme 13.

N to Rh. This result is in contrast to that derived from a monoanionic PCP ligand system. The reaction of 1,3-bis[(di-*tert*-butylphosphino)methyl]-2,4,6-trimethylbenzene with $[(C_2H_4)_2RhCl]_2$ in benzene at room temperature undergoes a selective C–C bond activation of aryl–methyl to produce $[\eta^3\text{-}C_6H(Me)_2(CH_2P^tBu_2)_2]Rh(Me)(Cl)$ accompanied by a competitive C–H activation of $ArCH_2$-H to give $[\eta^3\text{-}C_6H(Me)_2(CH_2P^tBu_2)_2CH_2]Rh(H)(Cl)$ [76], in which the latter ultimately isomerizes to become the former as the only thermodynamic product. The solid-state structures of both $\{Me[^i\text{Pr-PNP}^{Me}]\}RhCl$ and $[^i\text{Pr-PNP}^{Me}]Rh(Me)(Cl)$ were determined by X-ray crystallography [57], which revealed a distorted square-planar geometry for Rh in the former and square pyramidal for the latter (Fig. 9). Consistent with the trans influence, the methyl ligand in $[^i\text{Pr-PNP}^{Me}]Rh(Me)(Cl)$ occupies the apical position.

With an ethylene tether incorporated in the ligand backbone, the neutral $Me[^i\text{Pr-PNP}^{C2}]$ and monoanionic $[^i\text{Pr-PNP}^{C2}]^-$ ligands were anticipated to be more rigidly prearranged for meridional coordination to a metal. The reaction of $Me[^i\text{Pr-PNP}^{C2}]$ with $[(COD)RhCl]_2$ in aromatic solvents led ultimately to the formation of $[^i\text{Pr-PNP}^{C2}]Rh(Me)(Cl)$ [59]. The overall reaction proceeded much faster than that of $Me[^i\text{Pr-PNP}^{E}]$ under similar conditions, indicating that the ethylene-tethered ligand accelerates the N–C bond cleavage. Both $\{Me[^i\text{Pr-PNP}^{C2}]\}RhCl$ and $\{[^i\text{Pr-PNP}^{C2}]CH_2\}Rh(H)(Cl)$ were observed as intermediates spectroscopically. The observation of $\{[^i\text{Pr-PNP}^{C2}]CH_2\}Rh(H)(Cl)$ intermediate is reminiscent of that of $[\eta^3\text{-}C_6H(Me)_2(CH_2P^tBu_2)_2CH_2]Rh(H)(Cl)$ in the monoanionic PCP system [76]. Their conformations were supported by the experiments employing the $N^{13}CH_3$-labeled $Me[^i\text{Pr-PNP}^{C2}]$ compound, from which $\{Me[^i\text{Pr-PNP}^{C2}]\}RhCl$, $\{[^i\text{Pr-PNP}^{C2}]CH_2\}Rh(H)(Cl)$, and $[^i\text{Pr-PNP}^{C2}]Rh(Me)(Cl)$ were observed concurrently. Thus, the activation rates of C–H and C–N bonds in NMe of this ethylene-tethered ligand are likely comparable, in contrast to those found for the $Me[^i\text{Pr-PNP}^{E}]$ ligands where the C–H activation was not observed.

3.4.2. Iridium

The preparation of $[^i\text{Pr-PNP}^{Me}]Ir(H)(Cl)$ [57] was described as shown in Scheme 11. Thermolysis of an arene solution of $Me[^i\text{Pr-PNP}^{E}]$ (E = Me, F) and $[(COD)IrCl]_2$ at ca. 80 °C produced a mixture of products that contain $[^i\text{Pr-PNP}^{E}]Ir(Me)(Cl)$ and two isomers of $\{Me[^i\text{Pr-PNP}^{E}]^*\}Ir(H)(Cl)$ [59] as illustrated in Scheme 13. Attempts to observe the presumed $\{Me[^i\text{Pr-PNP}^{E}]\}IrCl$ intermediates (analogous to those shown in Scheme 12) were not successful. Instead, spectroscopic data of the reaction mixture at room temperature are indicative of the formation of an ionic compound that contains the $\{Me[^i\text{Pr-PNP}^{E}]\}Ir(\eta^4\text{-COD})^+$ cation, a consequence that is ascribed to the replacement of Cl^-, rather than COD, in $[(COD)IrCl]_2$ with the *N*-methylated diarylamido diphosphine ligand. Complexes $[^i\text{Pr-PNP}^{E}]Ir(Me)(Cl)$ were not isolated. Their identity anticipated from the N–C bond cleavage of the N–Me group was proposed by spectroscopic analogy with the corresponding rhodium counterparts. Recrystallization of the reaction mixture after thermolysis afforded one of the isomeric $\{Me[^i\text{Pr-PNP}^{E}]^*\}Ir(H)(Cl)$ suitable for X-ray analysis. The formation of $\{Me[^i\text{Pr-PNP}^{E}]^*\}Ir(H)(Cl)$ is apparently a result of C–H bond activation (or cyclometallation) of one of the isopropylmethyl groups, presumably from the unobserved $\{Me[^i\text{Pr-PNP}^{E}]\}IrCl$ intermediates. The four-membered iridacycle is severely strained and thus the coordination geometry about Ir is distorted from ideal octahedron. Nevertheless, the cyclometallated $\{Me[^i\text{Pr-PNP}^{E}]^*\}Ir(H)(Cl)$ complexes are air stable, consistent with the 18-electron count for these molecules.

The reaction of $Me[^i\text{Pr-PNP}^{C2}]$ with $[(COD)IrCl]_2$ in C_6D_6 at ambient temperature produced a mixture of $[^i\text{Pr-PNP}^{C2}]Ir(Me)(Cl)$, $\{Me[^i\text{Pr-PNP}^{C2}]^*\}Ir(H)(Cl)$, and $\{[^i\text{Pr-PNP}^{C2}]CH_2\}Ir(H)(Cl)$ [59]. None of the products was isolated. Employing the $N^{13}CH_3$-labeled $Me[^i\text{Pr-PNP}^{C2}]$ compound for this reaction assisted the characterization of these molecules. The formation of $\{Me[^i\text{Pr-PNP}^{E}]^*\}Ir(H)(Cl)$ and $\{Me[^i\text{Pr-PNP}^{C2}]^*\}Ir(H)(Cl)$ appears to suggest a higher preference for Ir than for Rh in a cyclometallation reaction.

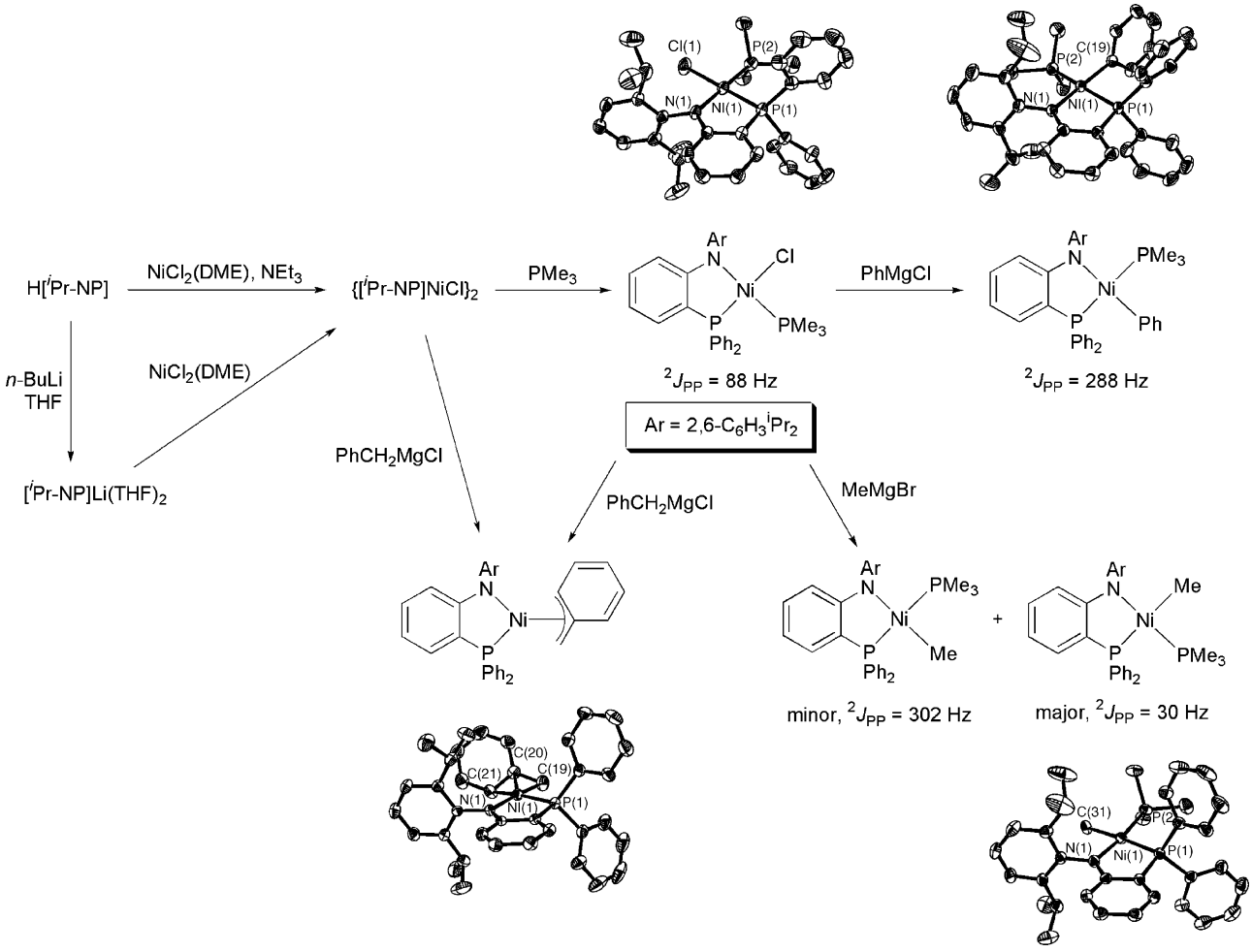

Scheme 14.

3.5. Group 10

3.5.1. Nickel

A series of diamagnetic nickel(II) complexes supported by bidentate diarylamido phosphine ligands, [^{i}Pr-NP]$^-$ and [Me-NP]$^-$, have been prepared [53]. The chloride complex, $\{[^i\text{Pr-NP}]\text{NiCl}\}_2$, is accessible from the reaction of either $NiCl_2$(DME) with [^{i}Pr-NP]Li(THF)$_2$ in THF at −35 °C or $NiCl_2$(DME) with H[^{i}Pr-NP] in THF at room temperature in the presence of triethylamine (Scheme 14). Analogous reactions employing sterically less demanding [Me-NP]$^-$ led likely to the concomitant formation of [Me-NP]$_2$Ni and the desired chloride complex, from which purification proved rather ineffective. Addition of PMe_3 to $\{[^i\text{Pr-NP}]\text{NiCl}\}_2$ afforded [^{i}Pr-NP]NiCl(PMe_3), from which [^{i}Pr-NP]NiMe(PMe_3), [^{i}Pr-NP]NiPh(PMe_3), and [^{i}Pr-NP]Ni(η^3-CH_2Ph) could be prepared from the metathetical reactions with appropriate Grignard reagents. In contrast, attempts to prepare well-defined η^1-alkyl or -aryl complexes from the reactions of $\{[^i\text{Pr-NP}]\text{NiCl}\}_2$ with a variety of Grignard reagents were not successful. Solution NMR data of [^{i}Pr-NP]NiMe(PMe_3) reveal two geometric isomers at room temperature with the major species carrying PMe_3 cis to the phosphorus donor of the amido phosphine ligand ($^2J_{pp}$ = 30 Hz). Interestingly, only one of the possible isomers was observed for [^{i}Pr-NP]NiCl(PMe_3) and [^{i}Pr-NP]NiPh(PMe_3), in which the two phosphorus donors in the former are exclusively cis ($^2J_{pp}$ = 88 Hz) whereas those in the latter are trans ($^2J_{pp}$ = 288 Hz). Similar to those found in H[^{i}Pr-NP] and [^{i}Pr-NP]Li(THF)$_2$, the isopropylmethyl groups in these nickel complexes are diastereotopic as evidenced by ^{1}H and ^{13}C NMR spectroscopy, implying restricted rotation about the N–Ar bond. These spectroscopic data are all consistent with the solid-state structures determined by X-ray crystallography.

Other than those illustrated in Scheme 14, the preparation of [^{i}Pr-NP]Ni(η^3-CH_2Ph) may also be accessible in 89% yield from the reaction of Ni(COD)$_2$ with $PhCH_2Cl$ in the presence of [^{i}Pr-NP]Li(THF)$_2$ (Scheme 15). This strategy takes advantage of facile oxidative addition of benzyl halides to zerovalent nickel [77] and avoids the prerequisite preparation of the chloride precursors, thereby providing a valuable entry to the sterically less bulky [Me-NP]$^-$ derivatives. The η^3 feature [78] of the benzyl ligand in these molecules maintained in solution was unambiguously elucidated by $^1J_{CH}$ of ca. 152 Hz observed for the benzylic methylene group in the NMR spectroscopy. The increased coupling constant, as compared to a typical value of 122 Hz for a normal sp^3 carbon atom, parallels a decreased Ni–C$_\alpha$–Ph

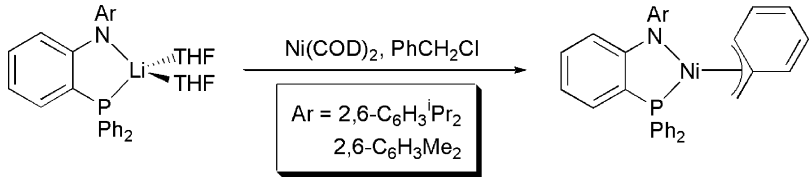

Scheme 15.

angle that leads to an increase in the amount of sp^2 character of the C_α atom [78,79]. The benzylic methylene group is exclusively cis to the phosphorus donor as indicated by the $^3J_{HP}$ value of 4 Hz and $^2J_{CP}$ of 9 Hz [80]. A rapid suprafacial rearrangement [81,82] of the η^3-benzyl ligand was proposed in solution on the basis of variable-temperature ^{1}H NMR studies. Both [^{i}Pr-NP]Ni(η^3-CH_2Ph) and [Me-NP]Ni(η^3-CH_2Ph) were characterized crystallographically [53].

Diamagnetic, square-planar nickel(II) complexes supported by tridentate amido diphosphine ligands were also prepared. The reactions of [R-PNP^E]Li(solv)$_n$ with $NiCl_2$(DME) in THF at −35 °C or those of H[R-PNP^E] with $NiCl_2(DME)_n$ (n = 0, 1) in the presence of triethylamine generated the corresponding [R-PNP^E]NiCl (Scheme 16) [23,54,83]. These chloride complexes are all air and water stable in both solution and solid state. Complexes [^{i}Pr-PNP^E]NiCl could also be prepared by heating a C_6D_6 solution of Me[^{i}Pr-PNP^E] (E = Me, F) and $NiCl_2$ at 90 °C [83], which involves cleavage of the N–Me bond in Me[^{i}Pr-PNP^E].

The chloride complexes [R-PNP^E]NiCl were found to react with $NaBH_4$ or a variety of Grignard reagents to afford [R-PNP^E]NiH and [R-PNP^E]NiR′, respectively [23,54,83]. The preparation of the nickel hydride complexes [R-PNP^E]NiH may be conveniently accessible by oxidative addition reactions of H[R-PNP^E] with Ni(COD)$_2$ [54,83]. Attempts to prepare [^{i}Pr-PNP^E]NiMe (E = Me, F) by the oxidative addition route of Me[^{i}Pr-PNP^E] with Ni(COD)$_2$ or Ni(PPh$_3$)$_4$ were not successful [83].

Of particular interest among the alkyl complexes isolated are those bearing β-hydrogen atoms [23,54] as analogous compounds were not reported in the closely related [N(SiMe$_2$CH$_2$PR$_2$)$_2$]$^-$ [84] and bidentate [NP]$^-$ [53] systems. Remarkably, these β-hydrogen-containing alkyl complexes are

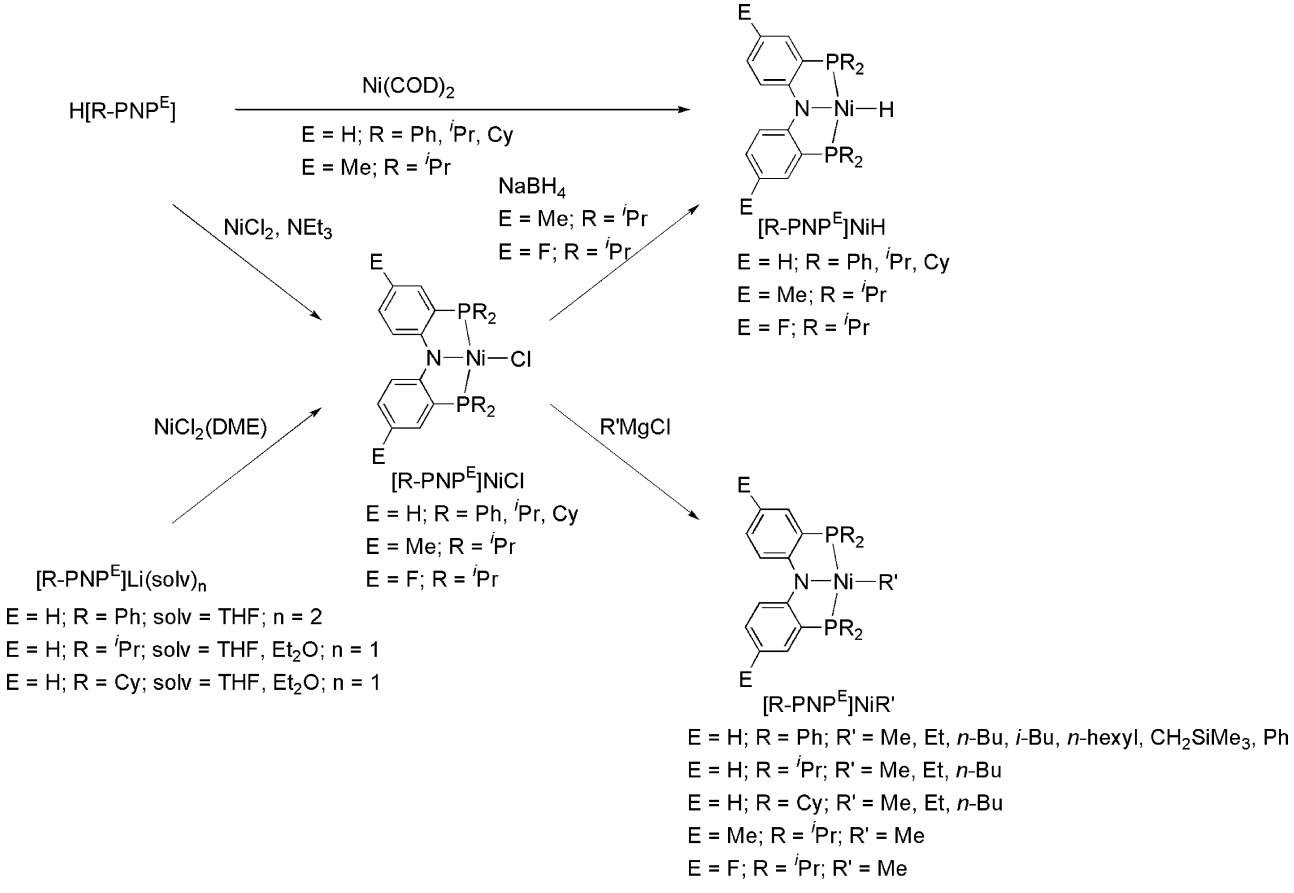

Scheme 16.

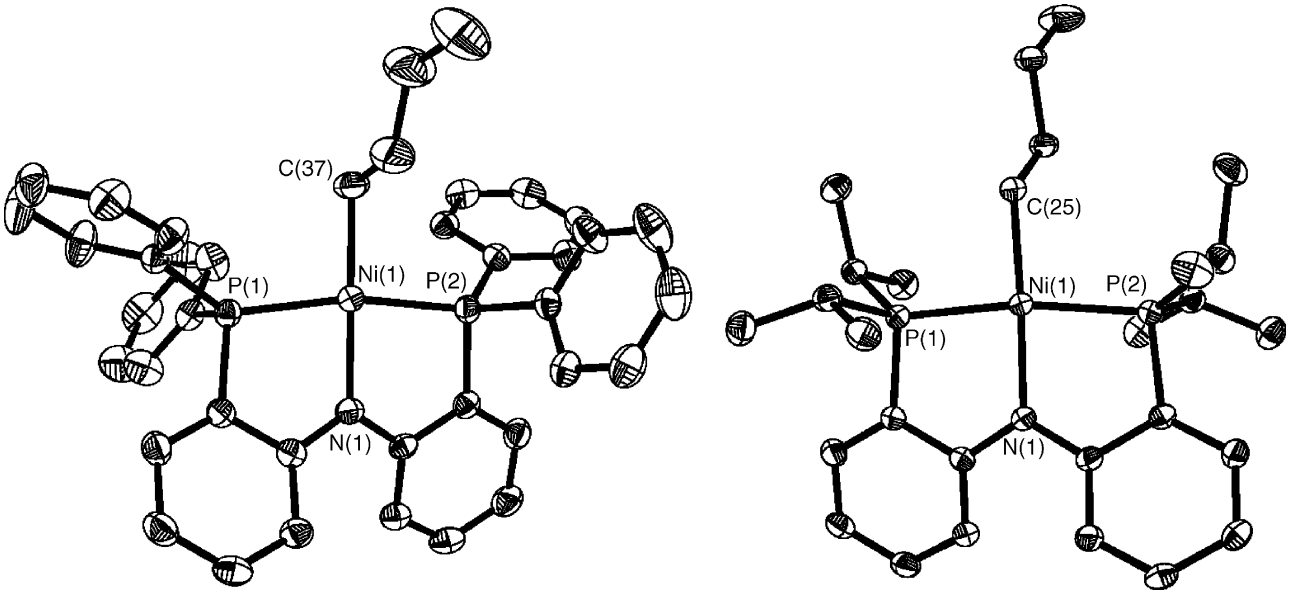

Fig. 10. Molecular structures of [Ph-PNP]Ni(*n*-Bu) (left) and [^{i}Pr-PNP]Ni(*n*-Bu) (right) established from X-ray studies [54].

thermally stable in benzene at 80 °C for >3 days, a result that is ascribed to the rigidity and robustness of the diarylamido diphosphine ligands, in which the dissociation of the phosphine arm(s), if any, cannot be significant. Fig. 10 depicts the X-ray structures of [Ph-PNP]Ni(*n*-Bu) and [^{i}Pr-PNP]Ni(*n*-Bu), which represent the rare examples of crystallographically characterized, mononuclear nickel complexes of acyclic alkyls that contain β-hydrogen atoms.[54] Interestingly, olefin insertion into the Ni–H bond of [Ph-PNP]NiH occurs readily, even at room temperature, to produce corresponding nickel hydrocarbyl complexes that contain β-hydrogen atoms. On the basis of these results and the principle of microscopic reversibility of β elimination and olefin insertion, it was proposed that the β elimination of [R-PNP]NiCH$_2$C*H*R′R″ species is likely uphill thermodynamically, at least for [Ph-PNP]$^{-}$ derivatives. These hydrocarbyl complexes were found to react with halogenated hydrocarbons such as dichloromethane, benzyl bromide, and phenyl iodide to generate the corresponding nickel halide derivatives, e.g., [Ph-PNP]NiX (X = Cl, Br, I) [54]. As a result, the chloride complexes [Ph-PNP]NiCl, [^{i}Pr-PNP]NiCl, and [Cy-PNP]NiCl were all active catalyst precursors for Kumada coupling reactions (Scheme 17), including those of alkyls containing β-hydrogen atoms [54], although the catalytic reaction conversion and selectivity were relatively unsatisfied. It should be noted that transition metal catalyzed cross-coupling reactions are usually incompatible with alkyl substrates that contain β-hydrogen atoms [85–87], which often suffer, at least in part, from facile β-hydrogen elimination. The electronic and steric modifications imposed by various substituents at the phosphorus donors in

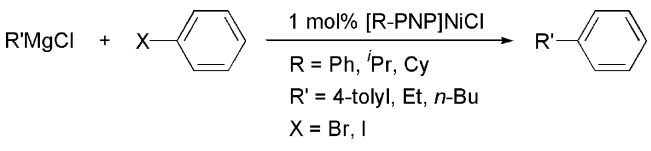

Scheme 17.

[Ph-PNP]NiCl, [^{i}Pr-PNP]NiCl, and [Cy-PNP]NiCl seem to have little impact on the catalytic activity.

Solution NMR data of these nickel complexes are all suggestive of a square-planar geometry for these molecules, with the amido diphosphine ligands being in a meridional coordination mode. The diagnostic evidence is the presence of virtual triplet resonances observed for the *o*-phenylene carbon atoms in the $^{13}C\{^{1}H\}$ NMR spectra. The H_α and C_α atoms in the hydrocarbyl complexes [R-PNP^{E}]NiR′ and the hydride ligand in [R-PNP^{E}]NiH were all observed as a triplet resonance in the ^{1}H and $^{13}C\{^{1}H\}$ NMR spectra. These spectroscopic data are consistent with the solid-state structures determined by X-ray crystallography where available. Consistent with the ionic sizes of divalent group 10 metals, the P–M–P angle decreases on going from [Ph-PNP]NiCl (171.72(4)°) [54] to [Ph-PNP]PdCl (165.27(11)°) [88] and [Ph-PNP]PtCl (167.30(8)°) [89].

3.5.2. Palladium

Palladium complexes of bi- and tridentate diarylamido phosphine ligands can be regarded as one of the electronic modifications of the popular phosphine palladacycles (Fig. 11) [31–33,36,90] that are active catalyst precursors for cross-coupling reactions. The metathetical reactions of [^{i}Pr-NP]Li(THF)$_2$ with PdCl$_2$(PhCN)$_2$ in THF at −35 °C produced {[^{i}Pr-NP]PdCl}$_2$ [91] in quantitative yield. Addition of PCy$_3$ to an ethereal solution of {[^{i}Pr-NP]PdCl}$_2$ generated quantitatively [^{i}Pr-NP]PdCl(PCy$_3$). Similar to that described in the nickel chemistry (Scheme 14) [53], the two phosphorous donors in [^{i}Pr-NP]PdCl(PCy$_3$) are mutually cis as indicated by the $^{2}J_{pp}$ value of 15 Hz. This result is consistent with that obtained from an X-ray diffraction study (Fig. 12) [91]. The isopropylmethyl groups in both {[^{i}Pr-NP]PdCl}$_2$ and [^{i}Pr-NP]PdCl(PCy$_3$) are diastereotopic, implying restricted rotation about the N–Ar bond for steric reason.

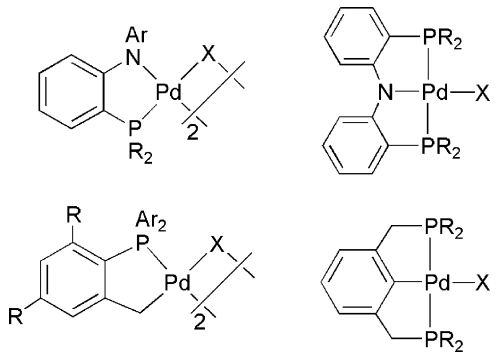

Fig. 11. Representative examples of phosphine palladacycles.

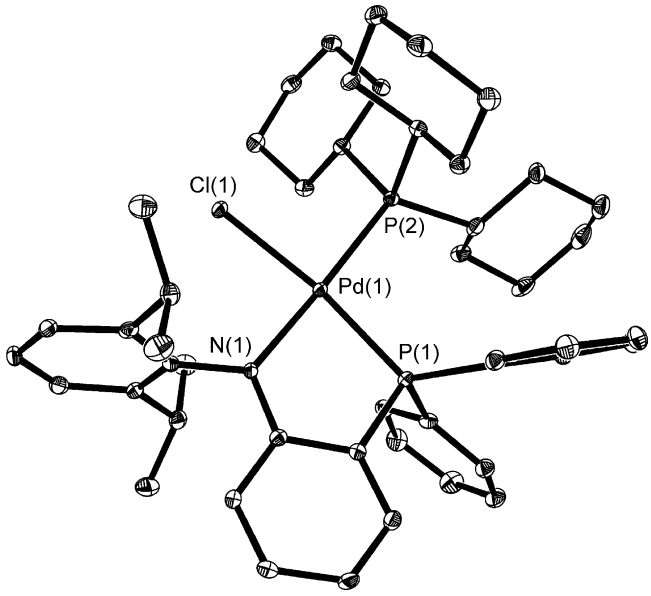

Fig. 12. Molecular structure of [^{i}Pr-NP]PdCl(PCy$_3$) established from an X-ray study [91].

The reactions of [Ph-PNP]Li(THF)$_2$ with PdCl$_2$(PhCN)$_2$ or Pd(OAc)$_2$ in THF at −35 °C produced [Ph-PNP]PdX (X = Cl, OAc) [88] quantitatively (Scheme 18). Alternatively, the analogous chloride and acetate complexes of [^{i}Pr-PNP^{E}]$^{-}$ (E = H, Me, F, Br, SiMe$_3$) may be prepared from the reactions of Me[^{i}Pr-PNP^{E}] or H[^{i}Pr-PNP^{Me}] with (COD)PdCl$_2$ or Pd(OAc)$_2$ [56,58,83]. Complex [^{i}Pr-PNP^{C2}]PdCl was prepared by heating a toluene solution of Me[^{i}Pr-PNP^{C2}] and (COD)PdCl$_2$ [59]. Mechanistic investigation was attempted for those involving N–Me bond cleavage by Pd(II) [58]. Though rather inconclusive, the mechanism may include either oxidative addition of the N–Me bond in the presumed {Me[^{i}Pr-PNP^{E}]}PdX$_2$ (X = Cl, OAc) intermediates or nucleophilic attack of X on the N*Me* group. Nevertheless, an intramolecular transformation of the presumed {Me[^{i}Pr-PNP^{Br}]}Pd(OAc)$_2$ intermediate to [^{i}Pr-PNP^{Br}]Pd(OAc) was determined at temperatures from 9 to 41 °C with activation parameters of $\Delta H^{\neq} = 23.5 \pm 1.5$ kcal mol^{-1}, $\Delta S^{\neq} = 3 \pm 5$ eu, and $\Delta G^{\neq}_{298} = 22.5 \pm 3.0$ kcal mol^{-1}. In contrast to these results that involve the selective cleavage of N–Me rather than NCH$_2$–H bond, only the ArCH$_2$–H activation product was reported for the thermolysis reaction of 1,3-bis[(dialkylphosphino)methyl]-2,4,6-trimethylbenzene (alkyl = ^{i}Pr, ^{t}Bu) with Pd(TFA)$_2$ (TFA = OCOCF$_3$) in THF at 80 °C [90]. Similar to those described in the nickel chemistry (Scheme 16), the palladium hydride and methyl complexes could also be prepared [83]. Solution NMR spectroscopic and X-ray crystallographic (where available) studies of these palladium complexes are all indicative of a square-planar geometry for these molecules. The crystallographic data are all suggestive of a weaker trans influence donor for amide in [PNP]$^{-}$ than for aryl carbanion in [PCP]$^{-}$. For instance, the

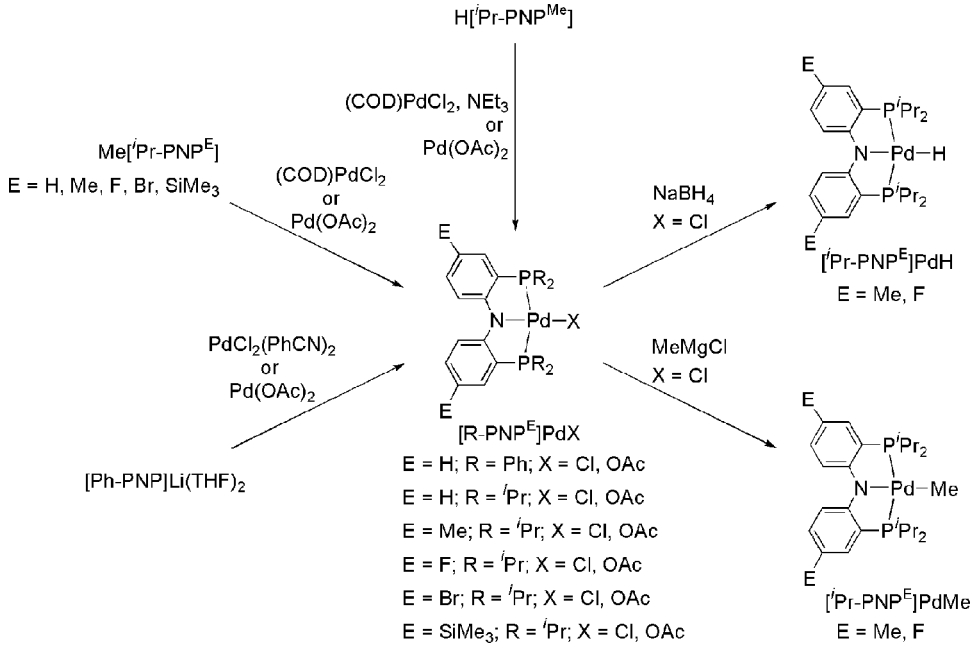

Scheme 18.

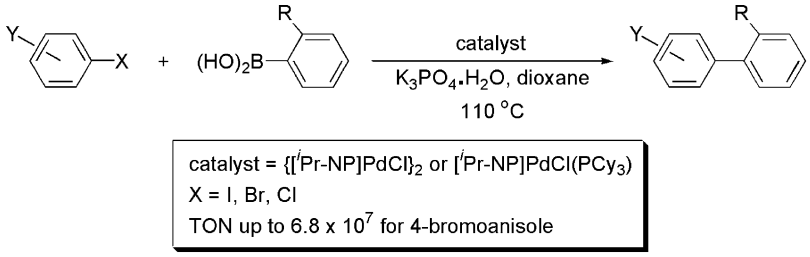

Scheme 19.

Pd–Cl distance of 2.313(5) Å in [Ph-PNP]PdCl [88] is similar to that of $[(Ph_2PCH_2SiMe_2)_2N]PdCl$ (2.3143(6) Å) [84] but notably shorter than that of $[\eta^3\text{-}2,6\text{-}(Ph_2PCH_2)_2C_6H_3]PdCl$ (2.367(3) Å) [92].

The palladium complexes $\{[^i\text{Pr-NP}]PdCl\}_2$, $[^i\text{Pr-NP}]PdCl(PCy_3)$, and [Ph-PNP]PdX (X = Cl, OAc) are all extremely thermostable at elevated temperatures (up to 200 °C) and not sensitive to air or water [88,91]. Of particular interest is perhaps their catalytic activity with respect to cross-coupling reactions.

In particular, catalytic Suzuki coupling reactions can be mediated by either $\{[^i\text{Pr-NP}]PdCl\}_2$ or $[^i\text{Pr-NP}]PdCl(PCy_3)$ (Scheme 19) for a wide array of electronically activated, unactivated, and deactivated aryl iodides, bromides, and chlorides [91]. A number of functional groups (e.g., nitro, ketone, aldehyde, halide, alkyl, alkoxy, etc.) are compatible with this catalytic condition. Consistent with the phenomenal stability of these palladium compounds, the coupling reactions can be conducted under aerobic conditions in the presence of water. Extremely high turnover numbers of up to 6.8×10^7 and turnover frequencies of up to 3.1×10^6 (per hour) were realized for the coupling of electronically deactivated 4-bromoanisole with phenylboronic acid. This catalytic condition also allows for the coupling of heterocyclic (e.g., 2-bromothiophene, 100% yield) and 2,6-disubstituted substrates. Of particular interest is the formation of tri-*ortho*-substituted biaryls (e.g., 2,2′,4,6-tetramethylbiphenyl, 82% yield) at efficient turnover rates. Kinetic studies on competitive experiments involving *p*-substituted aryl bromides led to Hammett plots with reaction constants ρ of 0.48 for $\{[^i\text{Pr-NP}]PdCl\}_2$ and 0.66 for $[^i\text{Pr-NP}]PdCl(PCy_3)$, implying that aryl halide oxidative addition is not the rate-determining step in this process. The low ρ values are similar to those reported for other catalytic Suzuki coupling reactions, in which transmetallation was suggested to be slow [93,94].

Palladium complexes of tridentate amido diphosphine ligands [Ph-PNP]$^-$ and $[^i\text{Pr-PNP}^{Me}]^-$ are active catalyst precursors for Heck olefination [56,88] of a variety of aryl iodides, bromides, and chlorides. Scheme 20 illustrates the catalytic reactions of aryl halides with styrene mediated by [Ph-PNP]PdX (X = Cl, OAc) [88]. A number of functional groups (e.g., nitro, ketone, aldehyde, halide, alkoxy, etc.) are compatible with this catalytic condition. Extraordinarily high turnover numbers of up to 4.5×10^7 and turnover frequencies of up to 1.1×10^6 (per hour) were achieved for the coupling of iodobenzene with styrene. Not surprisingly, the reactivity follows the order of iodide > bromide > chloride. Analogous to those found for the catalytic Suzuki coupling reactions [91], mechanistic studies on the Heck reactions outlined in Scheme 20 revealed a low reaction constant ρ of 0.60 [88], likely indicating that the rate-determining step is not the oxidative addition of the aryl–halide bond to the metal center of the active species. Similar observations were also reported for systems involving $[\eta^3\text{-}2,6\text{-}(^i\text{Pr}_2PCH_2)_2C_6H_3]PdX$ (X = trifluoroacetate, $\rho = 1.39$) [90] and related compounds [95], in which slow olefin coordination or insertion was suggested. The Heck coupling of aryl iodides and bromides with ethyl acrylate catalyzed by $[^i\text{Pr-PNP}^{Me}]PdX$ (X = Cl, OAc, H) was also reported [56].

3.5.3. Platinum

Platinum complexes of tridentate [Ph-PNP]$^-$ have been prepared and applied to promote intermolecular benzene C–H bond activation [89]. The reaction of [Ph-PNP]Li(THF)$_2$ with $PtCl_2(SMe_2)_2$ in THF at −35 °C produced [Ph-PNP]PtCl quantitatively. Subsequent reactions of [Ph-PNP]PtCl with MeMgCl, PhMgCl, or AgOTf afforded [Ph-PNP]PtMe, [Ph-PNP]PtPh, and [Ph-PNP]PtOTf, respectively. The methyl and phenyl complexes may be alternatively prepared by addition of H[Ph-PNP] at −35 °C to an ethereal solution of $[PtMe_2(\mu\text{-}SMe_2)]_2$ or *cis*-$PtPh_2(SMe_2)_2$, respectively. Protonolysis of [Ph-PNP]PtMe with HOTf also produced [Ph-PNP]PtOTf. The lability of the triflate ligand in [Ph-PNP]PtOTf was demonstrated by its facile displacement by pyridine and acetonitrile. Nevertheless, these platinum complexes are all thermally stable at elevated temperatures (150 °C), reminiscent of their nickel [23,54] and palladium [88] analogues. The solution NMR spectroscopic and X-ray crystallographic data are indicative of a square-planar geometry for these molecules.

Interestingly, treatment of a benzene solution of [Ph-PNP]PtMe with a stoichiometric amount of $B(C_6F_5)_3$ at room temperature led to the formation of [Ph-PNP]PtPh in quantitative yield (Scheme 21), a consequence that arises from the cleavage of a benzene C–H bond. Controlled experi-

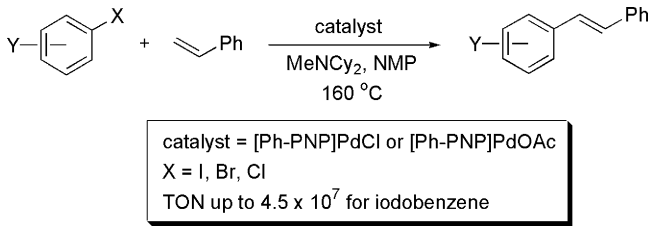

Scheme 20.

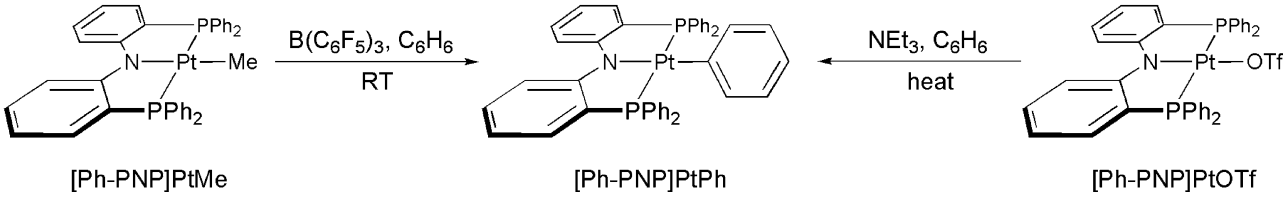

Scheme 21.

ments revealed that the conversion of [Ph-PNP]PtMe to [Ph-PNP]PtPh is proportional to the substoichiometry of $B(C_6F_5)_3$ employed, indicating a non-catalytic process for this reaction. Heating a benzene solution of [Ph-PNP]PtOTf to 110 °C or above in the presence of a variety of aliphatic amines (e.g., triethylamine, *N*-methyldicyclohexylamine ($MeNCy_2$), or 1,4-diazabicyclo[2.2.2]octane (DABCO)) yielded [Ph-PNP]PtPh quantitatively. In comparison, no reaction was found for [Ph-PNP]PtCl under similar conditions, suggesting that prior dissociation or displacement of the labile triflate ligand in [Ph-PNP]PtOTf is essential for the intermolecular benzene C–H bond activation in this process. A similar result was also reported for platinum triflate complexes supported by a monoanionic bis(8-quinolinyl)amide ligand [96].

Platinum complexes of $[^i\text{Pr-PNP}^E]^-$ (E = Me, F) were also attempted. Similar to those illustrated in Schemes 16 and 18, the reactions of $Me[^i\text{Pr-PNP}^E]$ (E = Me, F) or $H[^i\text{Pr-PNP}^{Me}]$ with $(COD)PtCl_2$ led to $[^i\text{Pr-PNP}^E]PtCl$, from which $[^i\text{Pr-PNP}^E]PtH$ and $[^i\text{Pr-PNP}^E]PtMe$ were prepared [83].

3.6. Group 11: copper

A dinuclear copper complex of $[^i\text{Bu-PNP}]^-$, $\{[^i\text{Bu-PNP}]Cu\}_2$ (Scheme 22), has been found to be an exceptionally efficient luminophore that exhibits both an exceptionally high quantum yield and a long lifetime [55]. This neutral, diamagnetic, luminescent yellow compound was prepared in 92% yield from either the metathetical reaction of $[^i\text{Bu-PNP}]Li$ with $CuBr(SMe_2)$ in diethyl ether or protonolysis of $H[^i\text{Bu-PNP}]$ with Cu(mesityl) (mesityl = 2,4,6-$C_6H_2Me_3$). The solid-state structure of $\{[^i\text{Bu-PNP}]Cu\}_2$ was characterized by X-ray crystallography, which revealed a short distance of 2.6245(8) Å for the two tetrahedral copper atoms in a Cu_2N_2 diamond core. When irradiated by visible light, $\{[^i\text{Bu-PNP}]Cu\}_2$ emits strongly in both solid state and solution. The quantum yield of this dicopper species at 298 K was determined: $\phi = 0.68 \pm 0.02$ in cyclohexane and 0.67 ± 0.04 in THF, and the lifetime of its excited state: $\tau = 10.2 \pm 0.2$ μs in cyclohexane and 10.9 ± 0.4 μs in THF. The unusual emission properties of $\{[^i\text{Bu-PNP}]Cu\}_2$ could be attributed to: (1) the relatively little structural reorganization [97] or ligand dissociation upon irradiation, and (2) the steric protection provided by the bulky amido diphosphine ligand for the two copper sites from solvent-induced exciplex formation [98]. Given the identification of two reversible redox couples at −550 and 300 mV in CH_2Cl_2 (referenced externally to the Fc^+/Fc couple) found for $\{[^i\text{Bu-PNP}]Cu\}_2$, this and related compounds may possibly lead to a photochemically driven multi-electron reaction process [99].

3.7. Group 12: zinc

The preparation of three-coordinate zinc complexes has been facilitated by the employment of a bidentate diarylamido phosphine ligand. The reaction of $H[^i\text{Pr-NP}]$ with ZnR_2 (R = Me, Et) in an ethereal solution at −35 °C produced $[^i\text{Pr-NP}]ZnR$ (Scheme 23) [28]. The isolation of monomeric, coordinatively unsaturated $[^i\text{Pr-NP}]ZnR$ is remarkable, particularly for *small alkyl* derivatives, as these reactions were conducted in strong coordinating solvents. Three-coordinate zinc complexes that are not associated with coordinating solvents are extremely rare

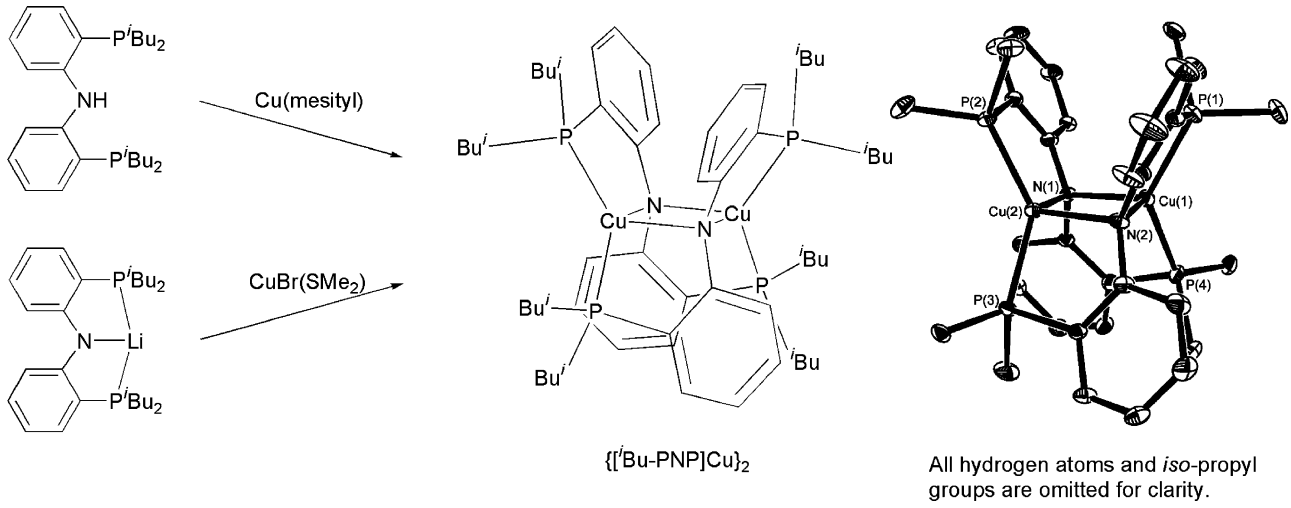

{[^{i}Bu-PNP]Cu}$_2$

All hydrogen atoms and *iso*-propyl groups are omitted for clarity.

Scheme 22.

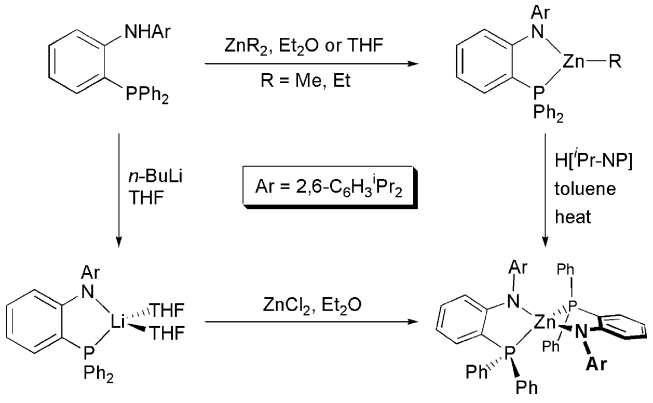

Scheme 23.

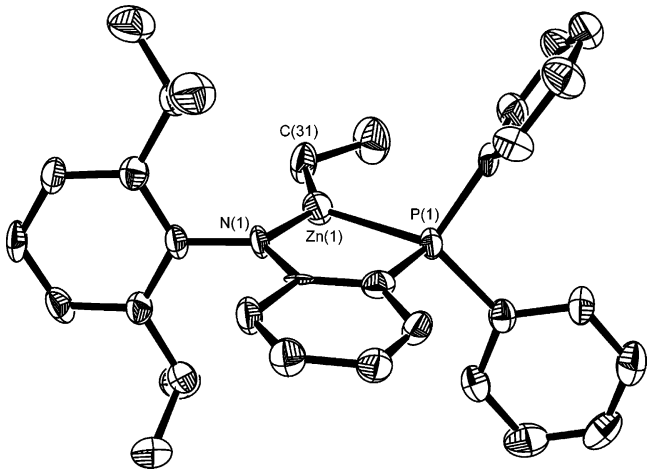

Fig. 13. Molecular structure of [^{i}Pr-NP]ZnEt established from an X-ray study [28].

[100]. Fig. 13 illustrates the X-ray structure of [^{i}Pr-NP]ZnEt. The isopropylmethyl groups in both [^{i}Pr-NP]ZnMe and [^{i}Pr-NP]ZnEt are diastereotopic as evidenced by solution NMR spectroscopic data, implying restricted rotation about the N–Ar bond due to the steric demand of the amido substituent. Complex [^{i}Pr-NP]ZnEt was characterized crystallographically.

The metathetical reaction of [^{i}Pr-NP]Li(THF)$_2$ with $ZnCl_2$ in diethyl ether at −35 °C generated the homoleptic [^{i}Pr-NP]$_2$Zn regardless of the stoichiometry employed. The bis-ligand complex [^{i}Pr-NP]$_2$Zn could also be prepared by heating a toluene solution of [^{i}Pr-NP]ZnR and H[^{i}Pr-NP] at 100 °C. No product formation was observed, however, when this reaction was performed at room temperature even after a prolonged period of time, due presumably to the significant steric repulsion between the two starting materials. Both X-ray crystallographic and solution NMR spectroscopic data of [^{i}Pr-NP]$_2$Zn are indicative of a tetrahedral geometry for the zinc center.

3.8. Group 13: aluminum

Aluminum complexes of bidentate diarylamido phosphine ligands were prepared. Alkane elimination reactions of H[Me-NP] with trialkylaluminum in toluene at 110 °C produced [Me-NP]AlR$_2$ (R = Me, Et) quantitatively (Scheme 24) [52]. High yields of [^{i}Pr-NP]AlMe$_2$ and [^{i}Pr-NP]AlEt$_2$ were obtained in a similar manner. Alternatively, the aluminum complexes could be accessible by metathetical reactions. Addition of one equiv of [Me-NP]Li(THF)$_2$ or [^{i}Pr-NP]Li(THF)$_2$ (either generated in situ or isolated) to $AlCl_3$ suspended in toluene at −35 °C cleanly produced [^{i}Pr-NP]AlCl$_2$ and [^{i}Pr-NP]AlCl$_2$. Subsequent alkylation of [Me-NP]AlCl$_2$ with two equiv of trimethylsilylmethyllithium in toluene at room temperature generated [Me-NP]Al(CH$_2$SiMe$_3$)$_2$. In contrast, attempted reaction of [^{i}Pr-NP]AlCl$_2$ with trimethylsilylmethyllithium (either one or two equiv) did not proceed at all under similar conditions, suggesting significant steric repulsion between [^{i}Pr-NP]$^-$ and trimethylsilylmethyl ligands. These aluminum complexes are extremely sensitive to air and moisture but stable, even at elevated temperatures, under an inert atmosphere for a prolonged period of time.

The solution structures of these four-coordinate aluminum dichloride and dialkyl derivatives were all determined by multinuclear NMR spectroscopy. The isopropylmethyl groups in the [^{i}Pr-NP]$^-$ derivatives are diastereotopic, again implying restricted N–Ar bond rotation in these molecules due to significant steric demand of the amido substituents. The ^{1}H NMR studies of [Me-NP]AlEt$_2$, [Me-NP]Al(CH$_2$SiMe$_3$)$_2$, and [^{i}Pr-NP]AlEt$_2$ are indicative of diastereotopic α-hydrogen atoms in these molecules. The chemical non-equivalence of the H$_\alpha$ atoms in Al–CH_2R fragments can be ascribable to the lack

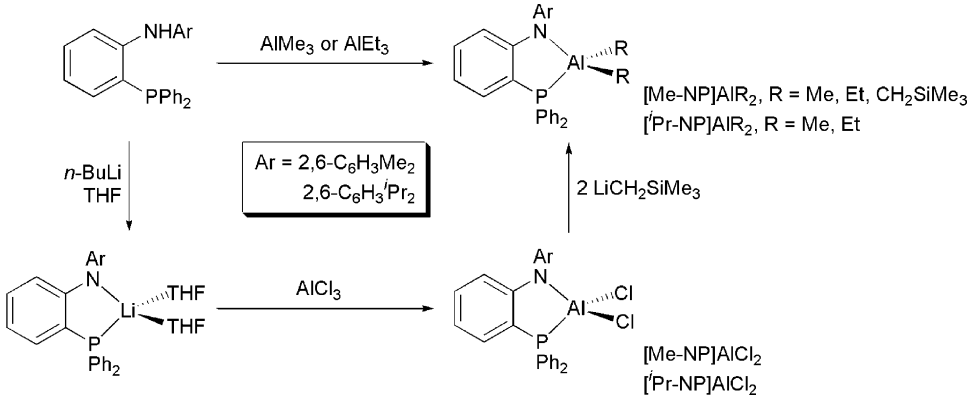

Scheme 24.

of symmetry of these molecules with respect to internal rotation involving the α-methylene groups [101]. Heteronuclear COSY and NOE experiments suggested that the phosphorus donor in [Me-NP]Al(CH_2SiMe_3)$_2$ and [^{i}Pr-NP]AlEt$_2$ is coupled to only one of the diastereotopic α-hydrogen atoms that is virtually antiperiplanar [102] with respect to the phosphorus atom. Conformations other than that found in [Me-NP]Al(CH_2SiMe_3)$_2$ and [^{i}Pr-NP]AlEt$_2$ may be accessible with sterically less demanding amido phosphine and/or alkyl ligands. Though sterically demanding, the phosphorus donor of [Me-NP]AlEt$_2$, [Me-NP]Al(CH_2SiMe_3)$_2$, and [^{i}Pr-NP]AlEt$_2$ does not dissociate readily even at high temperatures, as internuclear H_α–P coupling was found for these molecules at temperatures as high as 100 °C. This phenomenon highlights the rigidity of the *o*-phenylene backbone of the diarylamido phosphine ligands, in spite of the inherent mismatch of the hard aluminum and soft phosphorus atoms. The X-ray structures of [Me-NP]AlEt$_2$ and [^{i}Pr-NP]AlMe$_2$ were reported.

It has been well documented that the coordination number of neutral aluminum complexes correlates well with the chemical shifts of ^{27}Al ($I = 5/2$, natural abundance 100%) NMR spectroscopy [103]. All dialkyl complexes isolated in this study are not associated with coordinating solvents such as THF and diethyl ether, while the dichloride derivatives adopt THF readily, providing five-coordinate THF adducts [Me-NP]AlCl$_2$(THF) and [^{i}Pr-NP]AlCl$_2$(THF) as suggested by the ^{27}Al NMR spectroscopy and X-ray crystallography. Fig. 14 depicts the X-ray structure of [Me-NP]AlCl$_2$(THF) in which the aluminum center adopts a distorted trigonal bipyramidal geometry with the phosphorus donor and the coordinated THF molecule occupying axial positions. This result is in good agreement with a more electrophilic aluminum center of the four-coordinate dichloride complexes than that of their dialkyl counterparts (electronegativity: Cl, 3.16; C, 2.55) [104].

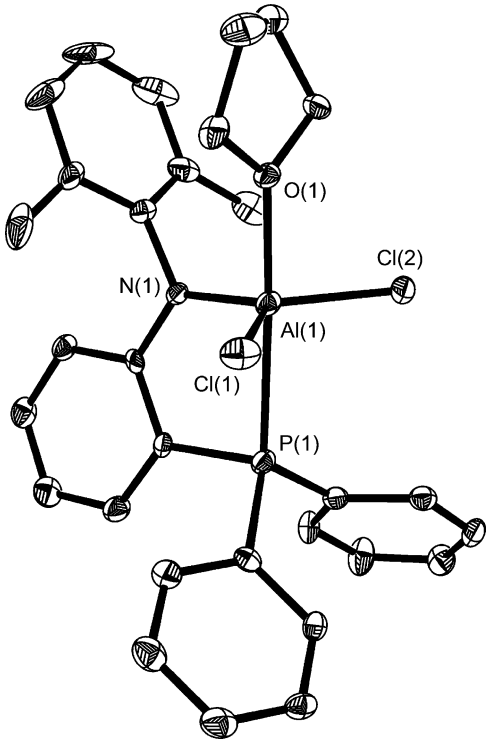

Fig. 14. Molecular structure of [Me-NP]AlCl$_2$(THF) established from an X-ray study [52].

4. Conclusions and perspectives

Though relatively young, chemistry involving metal complexes of chelating diarylamido phosphine ligands has become prosperous and versatile. With the incorporation of the *o*-phenylene backbone, the diarylamido phosphine ligands are significantly rigid and robust as has been demonstrated in the established coordination and organometallic chemistry. Given the versatility of the entire ligand set in view of variable hapticity (bi- and tridentate) and formal charge (mono- and dianionic), in combination with the availability of various substituents (alkyl and aryl) at the amido nitrogen and phosphorus donor atoms, the stability and reactivity of the diarylamido phosphine complexes may be finely tunable. Remarkably, catalytically active metal complexes that resist thermal decomposition at temperatures as high as 200 °C have been discovered [88]. A number of soft and hard main-group and transition metals have proven to be compatible, reflecting the hybrid characteristic of the diarylamido phosphine ligands. The chemistry developed thus far highlights the unusual reactivity (e.g., activation of inert chemical bonds [57,89], catalytic formation of carbon–carbon bonds [88,91], etc.) and stability (e.g., titanium phosphinidene [62], dinuclear copper luminophore [55], low coordinate zinc [28], etc.) of these molecules. On the basis of the results obtained to date, it is clear to foresee the possibility of a wide array of new diarylamido phosphine complexes and related compounds [105] that promise to engender exciting chemistry broadly and productively.

Acknowledgements

I thank the National Science Council of Taiwan for supporting research on this topic (NSC 94-2113-M-110-004 and NSC 93-2113-M-110-016) and the former and present undergraduate and graduate students who have dedicated their time and talent to this project. Acknowledgment is made to the National Center for High-performance Computing (NCHC) for the access to chemical databases.

References

[1] M.D. Fryzuk, J.B. Love, S.J. Rettig, V.G. Young, Science 275 (1997) 1445.
[2] M.D. Fryzuk, Can. J. Chem. 70 (1992) 2839.
[3] R.R. Schrock, S.W. Seidel, Y. Schrodi, W.M. Davis, Organometallics 18 (1999) 428.
[4] M.D. Fryzuk, S.A. Johnson, S.J. Rettig, J. Am. Chem. Soc. 120 (1998) 11024.
[5] M.D. Fryzuk, B.A. MacKay, B.O. Patrick, J. Am. Chem. Soc. 125 (2003) 3234.
[6] M.P. Shaver, M.D. Fryzuk, J. Am. Chem. Soc. 127 (2005) 500.
[7] M.D. Fryzuk, J.B. Love, S.J. Rettig, Chem. Commun. (1996) 2783.
[8] M.D. Fryzuk, J.B. Love, S.J. Rettig, Organometallics 17 (1998) 846.
[9] M.D. Fryzuk, G.R. Giesbrecht, S.J. Rettig, G.P.A. Yap, J. Organomet. Chem. 591 (1999) 63.

[10] M.D. Fryzuk, S.A. Johnson, S.J. Rettig, J. Am. Chem. Soc. 123 (2001) 1602.
[11] M.D. Fryzuk, C.M. Kozak, M.R. Bowdridge, W.C. Jin, D. Tung, B.O. Patrick, S.J. Rettig, Organometallics 20 (2001) 3752.
[12] M.D. Fryzuk, C.M. Kozak, P. Mehrkhodavandi, L. Morello, B.O. Patrick, S.J. Rettig, J. Am. Chem. Soc. 124 (2002) 516.
[13] M.D. Fryzuk, G.R. Giesbrecht, G. Olovsson, S.J. Rettig, Organometallics 15 (1996) 4832.
[14] M.D. Fryzuk, C.D. Montgomery, Coord. Chem. Rev. 95 (1989) 1.
[15] M.D. Fryzuk, T.S. Haddad, D.J. Berg, Coord. Chem. Rev. 99 (1990) 137.
[16] M.D. Fryzuk, S.A. Johnson, Coord. Chem. Rev. 200 (2000) 379.
[17] B.A. MacKay, M.D. Fryzuk, Chem. Rev. 104 (2004) 385.
[18] H. Basch, D.G. Musaev, K. Morokuma, M.D. Fryzuk, J.B. Love, W.W. Seidel, A. Albinati, T.F. Koetzle, W.T. Klooster, S.A. Mason, J. Eckert, J. Am. Chem. Soc. 121 (1999) 523.
[19] M.D. Fryzuk, B.A. Mackay, S.A. Johnson, B.O. Patrick, Angew. Chem. Int. Ed. 41 (2002) 3709.
[20] M.D. Fryzuk, M.P. Shaver, B.O. Patrick, Inorg. Chim. Acta 350 (2003) 293.
[21] O.V. Ozerov, H.F. Ferard, L.A. Watson, J.C. Huffman, K.G. Caulton, Inorg. Chem. 41 (2002) 5615.
[22] M.D. Fryzuk, T.S. Haddad, S.J. Rettig, Organometallics 10 (1991) 2026.
[23] L.-C. Liang, J.-M. Lin, C.-H. Hung, Organometallics 22 (2003) 3007.
[24] H.P. Fritz, I.R. Gordon, K.E. Schwarzhans, L.M. Venznzi, J. Chem. Soc. (1965) 5210.
[25] L. Crociani, F. Tisato, F. Refosco, G. Bandoli, B. Corain, Eur. J. Inorg. Chem. (1998) 1689, and references cited therein.
[26] D. Hedden, D.M. Roundhill, Inorg. Chem. 24 (1985) 4152.
[27] T.B. Rauchfuss, F.T. Patino, D.M. Roundhill, Inorg. Chem. 14 (1975) 652.
[28] L.-C. Liang, W.-Y. Lee, C.-H. Hung, Inorg. Chem. 42 (2003) 5471.
[29] A.M. Winter, K. Eichele, H.G. Mack, S. Potuznik, H.A. Mayer, W.C. Kaska, J. Organomet. Chem. 682 (2003) 149.
[30] R.G. Pearson, J. Chem. Educ. 45 (1968) 643.
[31] M. Beller, H. Fischer, W.A. Herrmann, K. Ofele, C. Brossmer, Angew. Chem. Int. Ed. 34 (1995) 1848.
[32] S. Gibson, D.F. Foster, G.R. Eastham, R.P. Tooze, D.J. Cole-Hamilton, Chem. Commun. (2001) 779.
[33] D. Morales-Morales, R. Redon, C. Yung, C.M. Jensen, Chem. Commun. (2000) 1619.
[34] M. Albrecht, G. van Koten, Angew. Chem. Int. Ed. 40 (2001) 3750.
[35] R.A. Gossage, L.A. Van De Kuil, G. Van Koten, Acc. Chem. Res. 31 (1998) 423.
[36] M.E. van der Boom, D. Milstein, Chem. Rev. 103 (2003) 1759.
[37] E. Peris, R.H. Crabtree, Coord. Chem. Rev. 248 (2004) 2239.
[38] M.Q. Slagt, D.A.P. van Zwieten, A. Moerkerk, R. Gebbink, G. van Koten, Coord. Chem. Rev. 248 (2004) 2275.
[39] N.J. Whitcombe, K.K. Hii, S.E. Gibson, Tetrahedron 57 (2001) 7449.
[40] R. Baumann, W.M. Davis, R.R. Schrock, J. Am. Chem. Soc. 119 (1997) 3830.
[41] R. Baumann, R. Stumpf, W.M. Davis, L.-C. Liang, R.R. Schrock, J. Am. Chem. Soc. 121 (1999) 7822.
[42] D.D. Graf, R.R. Schrock, W.M. Davis, R. Stumpf, Organometallics 18 (1999) 843.
[43] L.-C. Liang, R.R. Schrock, W.M. Davis, D.H. McConville, J. Am. Chem. Soc. 121 (1999) 5797.
[44] R.R. Schrock, F. Schattenmann, M. Aizenberg, W.M. Davis, Chem. Commun. (1998) 199.
[45] R.R. Schrock, J. Lee, L.-C. Liang, W.M. Davis, Inorg. Chim. Acta 270 (1998) 353.
[46] R.R. Schrock, L.-C. Liang, R. Baumann, W.M. Davis, J. Organomet. Chem. 591 (1999) 163.
[47] J.P. Wolfe, S. Wagaw, J.F. Marcoux, S.L. Buchwald, Acc. Chem. Res. 31 (1998) 805.
[48] J.F. Hartwig, Acc. Chem. Res. 31 (1998) 852.
[49] J.P. Sadighi, M.C. Harris, S.L. Buchwald, Tetrahedron Lett. 39 (1998) 5327.
[50] M.W. Haenel, S. Oevers, J. Bruckmann, J. Kuhnigk, C. Kruger, Synlett (1998) 301.
[51] M. Hingst, M. Tepper, O. Stelzer, Eur. J. Inorg. Chem. (1998) 73.
[52] L.-C. Liang, M.-H. Huang, C.-H. Hung, Inorg. Chem. 43 (2004) 2166.
[53] L.-C. Liang, W.-Y. Lee, C.-C. Yin, Organometallics 23 (2004) 3538.
[54] L.-C. Liang, P.-S. Chien, J.-M. Lin, M.-H. Huang, Y.-L. Huang, J.-H. Liao, Organometallics 25 (2006) in press.
[55] S.B. Harkins, J.C. Peters, J. Am. Chem. Soc. 127 (2005) 2030.
[56] L. Fan, B.M. Foxman, O.V. Ozerov, Organometallics 23 (2004) 326.
[57] O.V. Ozerov, C.Y. Guo, V.A. Papkov, B.M. Foxman, J. Am. Chem. Soc. 126 (2004) 4792.
[58] L. Fan, L. Yang, C.Y. Guo, B.M. Foxman, O.V. Ozerov, Organometallics 23 (2004) 4778.
[59] W. Weng, C.Y. Guo, C. Moura, L. Yang, B.M. Foxman, O.V. Ozerov, Organometallics 24 (2005) 3487.
[60] E.A. MacLachlan, M.D. Fryzuk, Organometallics 24 (2005) 1112.
[61] W. Weng, L. Yang, B.M. Foxman, O.V. Ozerov, Organometallics 23 (2004) 4700.
[62] B.C. Bailey, J.C. Huffman, D.J. Mindiola, W. Weng, O.V. Ozerov, Organometallics 24 (2005) 1390.
[63] F. Basuli, B.C. Bailey, J. Tomaszewski, J.C. Huffman, D.J. Mindiola, J. Am. Chem. Soc. 125 (2003) 6052.
[64] R.R. Schrock, Chem. Rev. 102 (2002) 145.
[65] F. Basuli, J. Tomaszewski, J.C. Huffman, D.J. Mindiola, J. Am. Chem. Soc. 125 (2003) 10170.
[66] P.-S. Chien, L.-C. Liang, Inorg. Chem. 44 (2005) 5147.
[67] M.D. Fryzuk, S.S.H. Mao, M.J. Zaworotko, L.R. Macgillivray, J. Am. Chem. Soc. 115 (1993) 5336.
[68] M.D. Fryzuk, P.B. Duval, S. Mao, S.J. Rettig, M.J. Zaworotko, L.R. MacGillivray, J. Am. Chem. Soc. 121 (1999) 1707.
[69] M.D. Fryzuk, P.B. Duval, S. Mao, M.J. Zaworotko, L.R. MacGillivray, J. Am. Chem. Soc. 121 (1999) 2478.
[70] R. Celenligil-Cetin, L.A. Watson, C.Y. Guo, B.M. Foxman, O.V. Ozerov, Organometallics 24 (2005) 186.
[71] L.A. Watson, J.N. Coalter, O. Ozerov, M. Pink, J.C. Huffman, K.G. Caulton, New J. Chem. 27 (2003) 263.
[72] C. Masters, B.L. Shaw, J. Chem. Soc. A (1971) 3679.
[73] G.M. Intille, Inorg. Chem. 11 (1972) 695.
[74] B.R. James, M. Preece, S.D. Robinson, Inorg. Chim. Acta 34 (1979) L219.
[75] M.A. Esteruelas, H. Werner, J. Organomet. Chem. 303 (1986) 221.
[76] B. Rybtchinski, A. Vigalok, Y. BenDavid, D. Milstein, J. Am. Chem. Soc. 118 (1996) 12406.
[77] T.J. Anderson, D.A. Vicic, Organometallics 23 (2004) 623.
[78] S.L. Latesky, A.K. McMullen, G.P. Niccolai, I.P. Rothwell, J.C. Huffman, Organometallics 4 (1985) 902.
[79] G.R. Giesbrecht, G.D. Whitener, J. Arnold, Organometallics 19 (2000) 2809.
[80] Z.J.A. Komon, X. Bu, G.C. Bazan, J. Am. Chem. Soc. 122 (2000) 12379.
[81] E. Carmona, M. Paneque, M. Poveda, Polyhedron 8 (1989) 285.
[82] R.R. Burch, E.L. Nuetterties, V.W. Day, Organometallics 1 (1982) 188.
[83] O.V. Ozerov, C.Y. Guo, L. Fan, B.M. Foxman, Organometallics 23 (2004) 5573.
[84] M.D. Fryzuk, P.A. Macneil, S.J. Rettig, A.S. Secco, J. Trotter, Organometallics 1 (1982) 918.
[85] M.R. Netherton, G.C. Fu, Adv. Synth. Catal. 346 (2004) 1525.
[86] T.-Y. Luh, M.-K. Leung, K.-T. Wong, Chem. Rev. 100 (2000) 3187.
[87] D.J. Cardenas, Angew. Chem. Int. Ed. 38 (1999) 3018.
[88] M.-H. Huang, L.-C. Liang, Organometallics 23 (2004) 2813.
[89] L.-C. Liang, J.-M. Lin, W.-Y. Lee, Chem. Commun. (2005) 2462.
[90] M. Ohff, A. Ohff, M.E. van der Boom, D. Milstein, J. Am. Chem. Soc. 119 (1997) 11687.
[91] L.-C. Liang, P.-S. Chien, M.-H. Huang, Organometallics 24 (2005) 353.

[92] F. Gorla, L.M. Venanzi, A. Albinati, Organometallics 13 (1994) 43.
[93] H. Weissman, D. Milstein, Chem. Commun. (1999) 1901.
[94] D. Zim, V.R. Lando, J. Dupont, A.L. Monteiro, Org. Lett. 3 (2001) 3049.
[95] F. Miyazaki, K. Yamaguchi, M. Shibasaki, Tetrahedron Lett. 40 (1999) 7379.
[96] S.B. Harkins, J.C. Peters, Organometallics 21 (2002) 1753.
[97] S.B. Harkins, J.C. Peters, J. Am. Chem. Soc. 126 (2004) 2885.
[98] D.R. McMillin, K.M. McNett, Chem. Rev. 98 (1998) 1201.
[99] A.G. Heyduk, D.G. Nocera, Science 293 (2001) 1639.
[100] J. Prust, A. Stasch, W. Zheng, H.W. Roesky, E. Alexopoulos, I. Usón, D. Böhler, T. Schuchardt, Organometallics 20 (2001) 3825.
[101] J.S. Waugh, F.A. Cotton, J. Phys. Chem. 65 (1961) 562.
[102] C.F. Tormena, M.P. Freitas, R. Rittner, R.J. Abraham, Magn. Reson. Chem. 40 (2002) 279.
[103] J.J. Delpuech, in: P. Laszlo (Ed.), NMR of Newly Accessible Nuclei, vol. 2, Academic Press, New York, 1983, p. 153.
[104] L. Pauling, The Nature of the Chemical Bond, third ed., Cornell University Press, Ithaca, NY, 1960, p. 93.
[105] W.-Y. Lee, L.-C. Liang, Dalton Trans. (2005) 1952.